



**HAL**  
open science

# Enhanced Pathogenesis Caused by Influenza D Virus and Mycoplasma bovis Coinfection in Calves: a Disease Severity Linked with Overexpression of IFN-gamma as a Key Player of the Enhanced Innate Immune Response in Lungs

Adrien Lion, Aurélie Secula, Camille Rançon, Olivier Boulesteix, Anne Pinard, Alain Deslis, Sara Hägglund, Elias Salem, Hervé Cassard, Katarina Näslund, et al.

## ► To cite this version:

Adrien Lion, Aurélie Secula, Camille Rançon, Olivier Boulesteix, Anne Pinard, et al.. Enhanced Pathogenesis Caused by Influenza D Virus and Mycoplasma bovis Coinfection in Calves: a Disease Severity Linked with Overexpression of IFN-gamma as a Key Player of the Enhanced Innate Immune Response in Lungs. Microbiology Spectrum, 2021, 9 (3), pp.e01690-21. 10.1128/spectrum.01690-21 . hal-03538899

**HAL Id: hal-03538899**

**<https://hal.inrae.fr/hal-03538899>**

Submitted on 21 Jan 2022

**HAL** is a multi-disciplinary open access archive for the deposit and dissemination of scientific research documents, whether they are published or not. The documents may come from teaching and research institutions in France or abroad, or from public or private research centers.


L'archive ouverte pluridisciplinaire **HAL**, est destinée au dépôt et à la diffusion de documents scientifiques de niveau recherche, publiés ou non, émanant des établissements d'enseignement et de recherche français ou étrangers, des laboratoires publics ou privés.



Distributed under a Creative Commons Attribution 4.0 International License



# Enhanced Pathogenesis Caused by Influenza D Virus and *Mycoplasma bovis* Coinfection in Calves: a Disease Severity Linked with Overexpression of IFN- $\gamma$ as a Key Player of the Enhanced Innate Immune Response in Lungs

Adrien Lion,<sup>a</sup> Aurélie Secula,<sup>a</sup> Camille Rançon,<sup>a</sup> Olivier Boulesteix,<sup>b</sup> Anne Pinard,<sup>b</sup> Alain Deslis,<sup>b</sup> Sara Hägglund,<sup>c</sup> Elias Salem,<sup>a</sup> Hervé Cassard,<sup>a</sup> Katarina Näslund,<sup>c</sup> Maria Gaudino,<sup>a</sup> Ana Moreno,<sup>d</sup> Emiliana Brocchi,<sup>d</sup> Maxence Delverdier,<sup>a</sup> Siamak Zohari,<sup>e</sup> Eric Baranowski,<sup>a</sup> Jean-François Valarcher,<sup>c</sup> Mariette F. Ducatez,<sup>a</sup>  Gilles Meyer<sup>a</sup>

<sup>a</sup>IHAP, UMR1225, Université de Toulouse, INRAE, Ecole Vétérinaire de Toulouse, Toulouse, France

<sup>b</sup>INRAE, UE 1277, Experimental Infectiology Platform (PFIE), INRA-Val de Loire Research Centre, Nouzilly, France

<sup>c</sup>Swedish University of Agricultural Sciences, Host Pathogen Interaction Group, Department of Clinical Sciences, Uppsala, Sweden

<sup>d</sup>Istituto Zooprofilattico Sperimentale Della Lombardia e dell'Emilia Romagna Bruno Ubertini, Brescia, Italy

<sup>e</sup>Department of Virology, Immunobiology and Parasitology, National Veterinary Institute, Uppsala, Sweden

**ABSTRACT** Bovine respiratory disease (BRD) is a major disease of young cattle whose etiology lies in complex interactions between pathogens and environmental and host factors. Despite a high frequency of codetection of respiratory pathogens in BRD, data on the molecular mechanisms and pathogenesis associated with viral and bacterial interactions are still limited. In this study, we investigated the effects of a coinfection with influenza D virus (IDV) and *Mycoplasma bovis* in cattle. Naive calves were infected by aerosol with a French IDV strain and an *M. bovis* strain. The combined infection shortened the incubation period, worsened the disease, and led to more severe macroscopic and microscopic lesions compared to these parameters in calves infected with only one pathogen. In addition, IDV promoted colonization of the lower respiratory tract (LRT) by *M. bovis* and increased white cell recruitment to the airway lumen. The transcriptomic analysis highlighted an upregulation of immune genes in the lungs of coinfecting calves. The gamma interferon (IFN- $\gamma$ ) gene was shown to be the gene most statistically overexpressed after coinfection at 2 days postinfection (dpi) and at least until 7 dpi, which correlated with the high level of lymphocytes in the LRT. Downregulation of the PACE4 and TMPRSS2 endoprotease genes was also highlighted, being a possible reason for the faster clearance of IDV in the lungs of coinfecting animals. Taken together, our coinfection model with two respiratory pathogens that when present alone induce moderate clinical signs of disease was shown to increase the severity of the disease in young cattle and a strong transcriptomic innate immune response in the LRT, especially for IFN- $\gamma$ .

**IMPORTANCE** Bovine respiratory disease (BRD) is among the most prevalent diseases in young cattle. BRD is due to complex interactions between viruses and/or bacteria, most of which have a moderate individual pathogenicity. In this study, we showed that coinfection with influenza D virus (IDV) and *Mycoplasma bovis* increased the severity of the respiratory disease in calves in comparison with IDV or *M. bovis* infection. IDV promoted *M. bovis* colonization of the lower respiratory tract and increased white cell recruitment to the airway lumen. The transcriptomic analysis highlighted an upregulation of immune genes in the lungs of coinfecting calves. The IFN- $\gamma$  gene in particular was highly overexpressed after coinfection, correlated with the disease severity, immune response, and white cell recruitment in the lungs. In conclusion, we showed that IDV facilitates coinfections within the BRD complex by modulating

**Editor** Frederick S. B. Kibenge, University of Prince Edward Island

**Copyright** © 2021 Lion et al. This is an open-access article distributed under the terms of the [Creative Commons Attribution 4.0 International license](https://creativecommons.org/licenses/by/4.0/).

Address correspondence to Gilles Meyer, gilles.meyer@envt.fr.

The authors declare no conflict of interest.

**Received** 29 September 2021

**Accepted** 23 November 2021

**Published** 22 December 2021

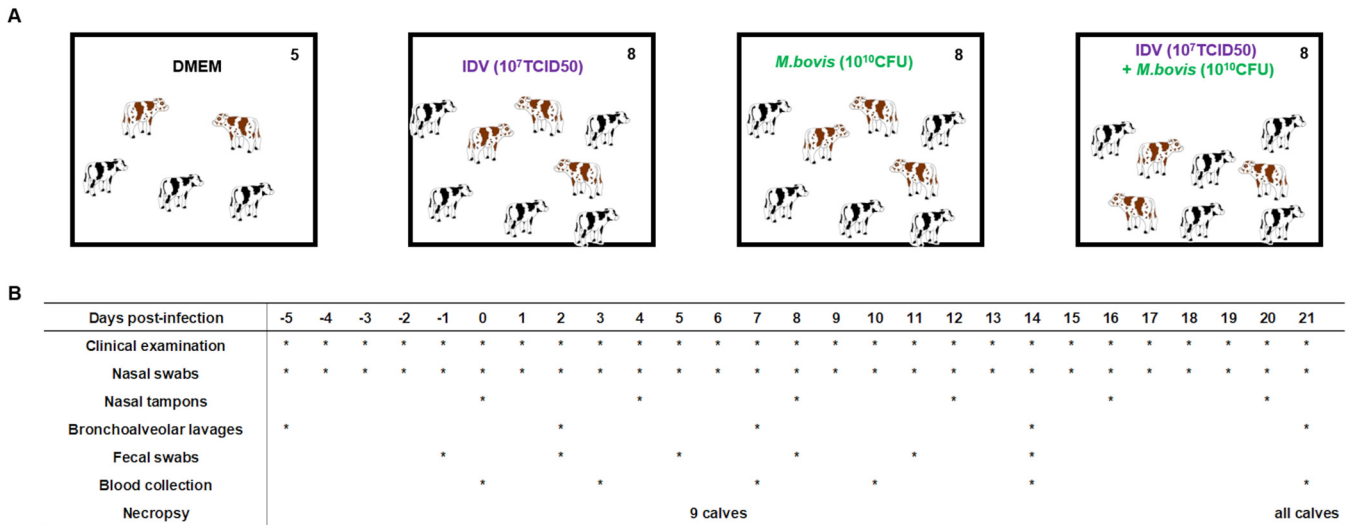
the local innate immune response, providing new insights into the mechanisms involved in severe respiratory diseases.

**KEYWORDS** influenza D virus, *Mycoplasma bovis*, cattle, bovine respiratory disease, coinfection, immune response

**B**ovine respiratory disease (BRD) is among the most prevalent pathological conditions in young cattle, resulting in poor animal welfare, significant economic losses, and increased antibiotic use in livestock (1). BRD is a multifactorial disease, resulting from complex interactions between pathogens and environmental and host factors, which can result in severe or fatal bronchopneumonia. Its complexity is often enhanced by the presence of mixed infections involving bacteria and viruses. The most important respiratory viruses involved in BRD are bovine respiratory syncytial virus (BRSV), bovine parainfluenza type 3 virus (BPIV-3), bovine viral diarrhoea virus (BVDV), bovine coronavirus (BCoV), and sometimes bovine herpesvirus type 1 (BoHV1). *Mannheimia haemolytica*, *Pasteurella multocida*, *Histophilus somni*, and *Mycoplasma bovis* are the most common bacteria found and described in BRD (2). Among all pathogens, BRSV and *M. haemolytica* are considered major agents due to their ability to reproduce severe respiratory clinical signs when experimentally inoculated into naive calves (3, 4). In addition, recent metagenomics studies using next-generation sequencing (NGS) suggest a very high frequency of coinfections in BRD and have made it possible to identify new pathogens that are potentially involved (2, 5–9). These coinfections include well known respiratory pathogens but also viruses for which pathogenicity has not been demonstrated. For example, in North American BRD cases, coinfections frequently occurred between influenza D virus (IDV), BCoV, and bovine rhinitis A and B viruses (BRAV and BRBV, respectively) (5–7). Among these, IDV was isolated for the first time in 2011 in the United States from a swine exhibiting influenza-like syndrome (10). Despite its first detection in a pig, epidemiological studies highlighted a limited diffusion of IDV infection in this species. The high prevalence of IDV in cattle suggests this species as IDV's main host (11–16). Alone, IDV induced only mild respiratory clinical signs in experimentally infected naive calves, despite replication in both the upper respiratory tract (URT) and lower respiratory tract (LRT) (17, 18). Metagenomics approaches suggested that IDV was implicated in BRD when associated with classical pathogens and/or with less known viruses, such as BRAV, BRBV, bovine nidovirus (BNV), bovine astrovirus (BAV), and bovine adenovirus type 3 (BAV-3) (6–8).

Primary viral infections are well known to predispose the respiratory tract to secondary bacterial infections that lead to respiratory complications (19–21). Recent studies have shown that viral infection can promote bacterial superinfection but also that preexisting bacterial infections can promote viral shedding (20, 22). We recently identified frequent codetection of IDV and *M. bovis* in cattle with clinical respiratory signs on French veal farms (M. Gaudino, M.F. Ducattez, G. Meyer, personal communication) and Canadian dairy farms (23). Our field surveillance indicates that both IDV and *M. bovis* infections occurred at the same time, just after calves' allocation, suggesting that *M. bovis* and IDV may act together as primary disease pathogens (Gaudino et al., personal communication). And yet, many cases of *M. bovis* are coinfections with other bacteria or viruses, as already suggested (24, 25).

To date, only one IDV and only one *M. bovis* experimental coinfection study have been performed in cattle. The first study suggested that primary IDV infection does not increase the clinical signs and susceptibility to secondary bacterial infection with *M. haemolytica* in calves (26). The second one explored the influence of BoHV-1 or BVDV type 2 primary infection on *M. bovis* superinfection in a calf model by modulating inoculation routes and doses (27). The authors showed that only calves first infected with BoHV-1 developed the respiratory disease after infection with *M. bovis*. As the association between *M. bovis* and IDV was observed in French veal calves and Canadian dairy cows with respiratory clinical signs, we assessed here whether this association of



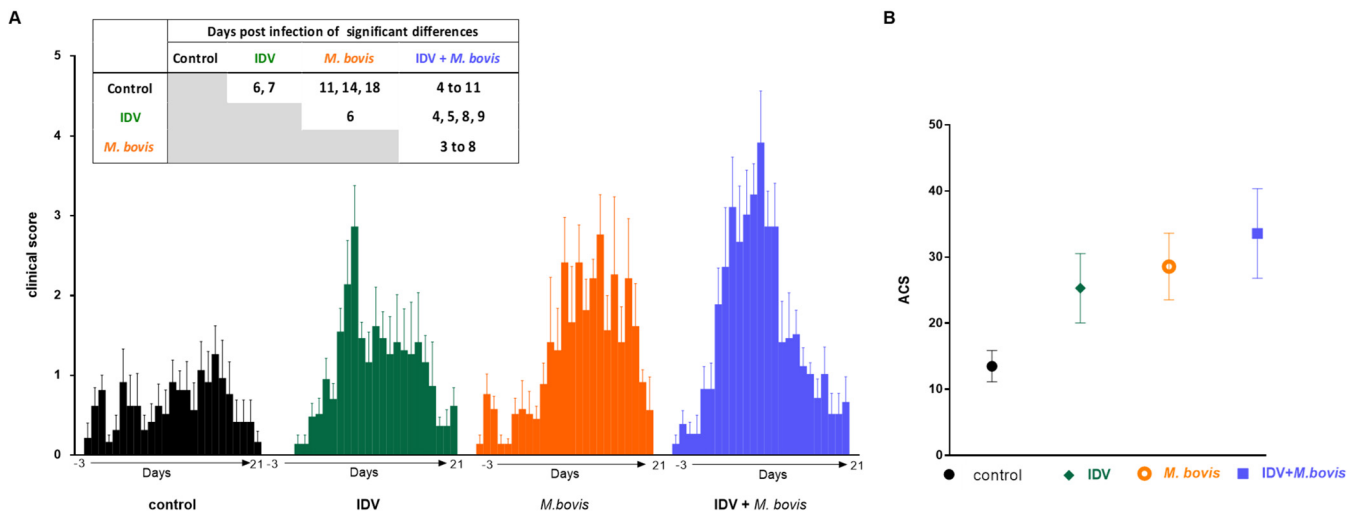


**FIG 2** The coinfection increases the clinical scores. (A) Mean clinical scores with significant differences between groups. (B) Mean accumulated clinical score (ACS) for each group.

group, at  $5 \pm 1.6$  days, with a peak at day  $8.6 \pm 1.3$  and duration of CS of  $9.8 \pm 2.5$  days. Two calves had substantial clinical signs (SCS values of 39 and 58), with loss of appetite, general state impairment, decubitus, increased respiratory rate (30 to 60 breaths/min), mucopurulent discharge, numerous episodes of spontaneous cough, and abnormal lung sounds. For the other three calves, clinical signs were similar but less intense (SCS values of 20.5, 23.2, and 28.2). All animals had recovered by 21 dpi except one, which was still slightly ill.

The average CS and the mean of the individual areas under the curves of daily clinical scores (ACS) with statistical differences are shown in Fig. 2. Significant differences in CS were detected between controls and coinfecting (IDV+*M. bovis*-infected) calves from 4 to 11 dpi ( $0.0001 < P < 0.05$ ) (Fig. 2A). The coinfecting calves also showed statistical differences with the IDV-infected calves at 4, 5, 8, and 9 dpi but not at 6 and 7 dpi, which corresponds to the maximum of the CS of IDV-infected calves (statistical differences with the control calves). In addition, statistical differences were observed from 3 to 8 dpi between the coinfecting and *M. bovis*-infected calves. Higher severity of disease in the coinfecting calves was also detected when the mean areas under the curve (AUCs) of clinical scores were compared (Fig. 2B), although no statistical significance could be observed.

**Macroscopic and microscopic lesions were more severe in the coinfecting calves than in IDV- or *M. bovis*-infected calves.** To evaluate the gross lesions, animals were euthanized at 6 dpi (three animals per infected group) and 21 dpi (remaining calves). No gross lesions were found in control animals, either at 6 dpi or at 21 dpi (Fig. 3A). Similar to a previous study of experimental infection with IDV (18), only a single animal (9242) displayed minor macroscopic lung lesions of atelectasis and interstitial pneumonia at 6 dpi, covering 5 to 10% of the right cranial and accessory lobe surfaces (Fig. 3B). In the *M. bovis*-infected calves, no gross lesions were found at 6 dpi (Fig. 3C), and two calves (9697 and 9249) euthanized at 21 dpi had moderate lesions of nasal congestion and subacute interstitial bronchopneumonia, respectively. Remarkably, the main gross lesions were observed in the coinfecting calves at 6 dpi. Two calves (9709 and 9718) had lesions of severe tracheitis with foci of necrosis and a fibrinopurulent exudate on the mucosal surface (Fig. 3D). The third calf (9239) had interstitial pneumonia with atelectasis of 30% of the cranial and accessory lobe surfaces. The latter calf did not harbor lesions on the trachea. At 21 dpi, three (9700, 9241, and 9244) and four (9700, 9705, 9241, and 9244) of five coinfecting calves had lesions of tracheitis and acute interstitial pneumonia of minimal extent (5 to 10%), respectively. No other macroscopic lesions were observed in the other systems (digestive, nervous, urinary, etc.) of the 29 calves used in this experiment.



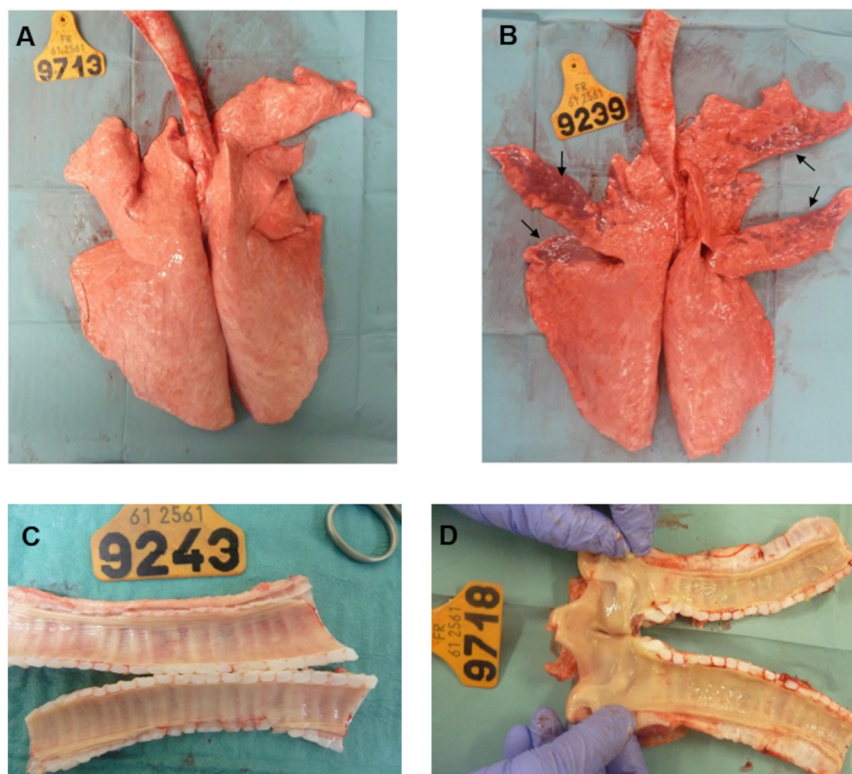


**FIG 3** Types of macroscopic lesions observed. Macroscopic lesions in respiratory organs in infected compared to control animals. (A) Lung without macroscopic lesions of control calf 9713. (B) Thirty percent of the cranial and accessory lobes of the coinfecting animal 9239 had atelectasis (arrows). (C) No gross lesions were observed at 6 dpi on the trachea of calf 9243 infected by *M. bovis*. (D) Tracheitis lesions with a fibrinopurulent exudate were observed on the mucosal surface of coinfecting calf 9718 at 6 dpi.

At 6 dpi, microscopic lesions were only found in respiratory tissues (Fig. 4 and 5). The three IDV-infected animals had microscopic lesions in the nasal cavities and/or trachea, characterized by loss of cilia, necrosis and exfoliation of the superficial mucosal epithelium, and infiltration of the lamina propria by mononuclear cells (Fig. 4). All coinfecting calves euthanized at 6 dpi showed lesions of rhinitis and tracheitis similar to those of IDV-infected calves, except that these lesions were more pronounced in the trachea (Fig. 5). Only coinfecting calf 9709 had light microscopic lesions of subacute bronchointerstitial pneumonia in the left cranial lung lobe, characterized by neutrophils in the bronchial lumens, neutrophilic and macrophagic alveolitis, and peribronchial and septal lymphoplasmocytic infiltration in the lung. No microscopic lesions were found in animals infected by *M. bovis* and euthanized at 6 dpi. The macroscopic lesions observed at 21 dpi were not analyzed by histology.

**IDV and *M. bovis* coinfection increases white cell recruitment to the airway lumen.** To analyze the white cell response in the lung, the cellular compositions of BAL fluid samples at 2, 7, and 14 dpi were determined by using a cytopspin system and May-Grünwald Giemsa (MGG) staining. Whole immune cells, macrophages, neutrophils, and lymphocytes from the different samples were counted (Table 1).

In the control calves, the mean whole immune cell count (WCC) and neutrophil and macrophage counts remained stable during the study. However, a small progressive increase in the lymphocyte mean count was detected in control calves between 2 and 14 dpi (Table 1).

In the IDV-infected calves, the mean WCCs were higher at 7 and 14 dpi than at 2 dpi. This increase was mainly due to the maintenance of a high number of macrophages and an increase in neutrophil recruitment (26.3% increase between 2 and

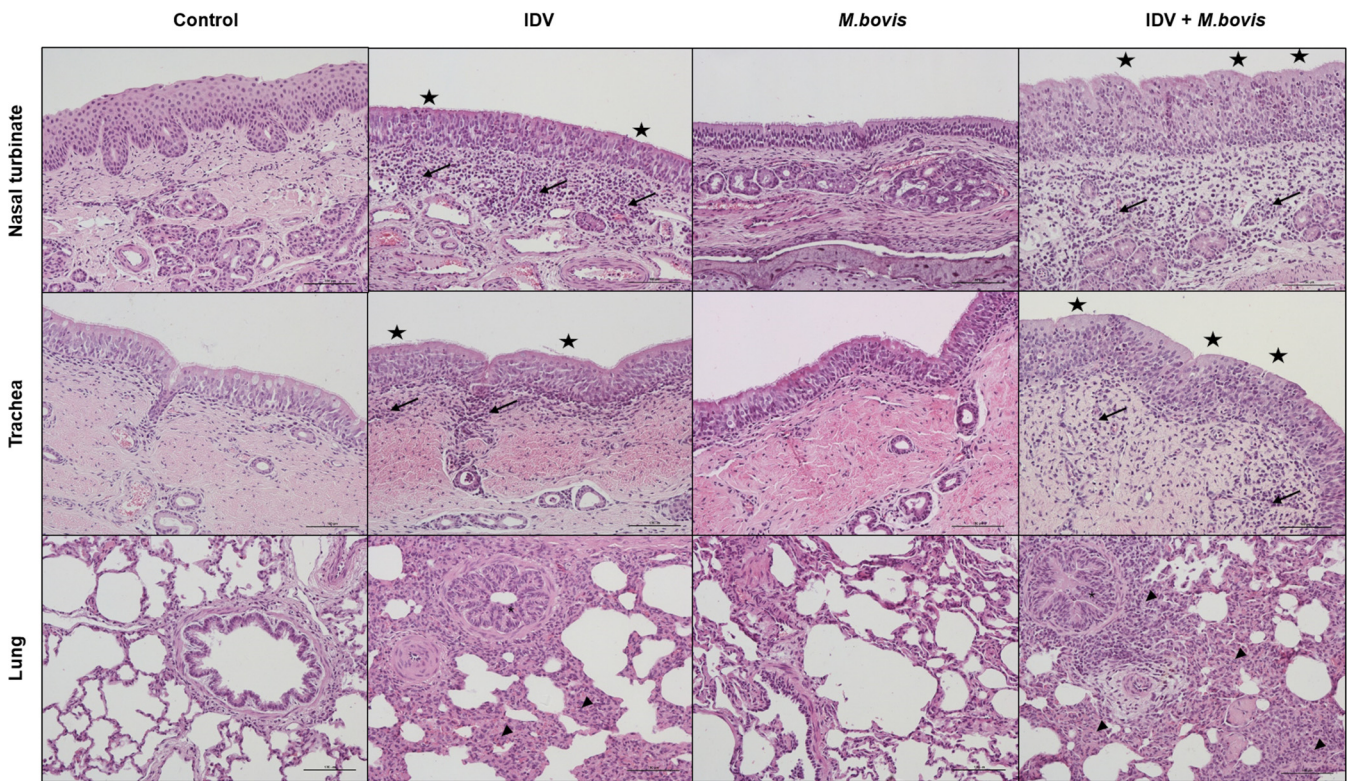


**FIG 4** The coinfection induced greater lesions in the respiratory organs than did mono-infection. Hematoxylin and eosin staining of nasal turbinate (top), trachea (middle), and lung (bottom) tissue samples at 6 dpi. Magnification,  $\times 200$ ; scale bars,  $100\ \mu\text{m}$ . H&E-stained sections demonstrating a loss of ciliature and necrosis and exfoliation of the superficial mucosal epithelium (stars), an infiltration of the lamina propria by mononuclear cells (arrows), subacute bronchointerstitial pneumonia with neutrophils in bronchial lumens (asterisk), and neutrophilic and macrophagic alveolitis and peribronchial and septal lymphoplasmacytic infiltration (arrowheads).

7 dpi). The mean lymphocyte counts were also higher at 7 and 14 dpi than at 2 dpi. However, the percentage of lymphocytes over other white cell types was higher at 2 dpi than later during infection. Moreover, compared to the control calves, the IDV-infected calves tended to have a higher level of lymphocytes at 2 dpi (0.2% versus 1.2%) (Table 1).

In the *M. bovis*-infected calves, the WCCs tended to differ between 2 and 7 dpi or 2 and 14 dpi, mainly due to the increases in the neutrophil fraction, with a 23.2% and a 4.9% increase, respectively. The numbers of lymphocytes increased between 2 and 7 dpi and between 2 and 14 dpi, with 0.3% and 1.4% increases, respectively (Table 1).

In the IDV+*M. bovis*-infected calves, compared to the control calves, the mean WCC tended to be increased at 2 dpi mainly due to the high level of the neutrophil count (23.4%). The most significant change for the coinfecting calves was observed at 7 dpi, when the WCC was increased by 1.6-fold compared to its level at 2 dpi, while it did not change in the controls between these two time points. The diapedesis of neutrophils into the lumen of the airways (14.9% increase in neutrophils in BAL fluid samples between 2 and 7 dpi) was mainly responsible for this increase of the WCC in the coinfecting calves, while the number of macrophages was relatively stable between these two time points. The fraction of lymphocytes increased by 1.0% between 2 and 7 dpi. At 14 dpi, the WCC returned to the initial state in the coinfecting calves; however, the neutrophil and lymphocyte fractions remained high, while the percentage of macrophages was reduced by 3.5% compared to the percentage at 2 dpi (Table 1).

Due to the individual variations, none of the differences in white cell-type counts were statistically significant.

**IDV infection promotes *M. bovis* colonization of the URT.** To assess the shedding of IDV in the URT, the presence of IDV RNA was monitored by reverse-transcriptase

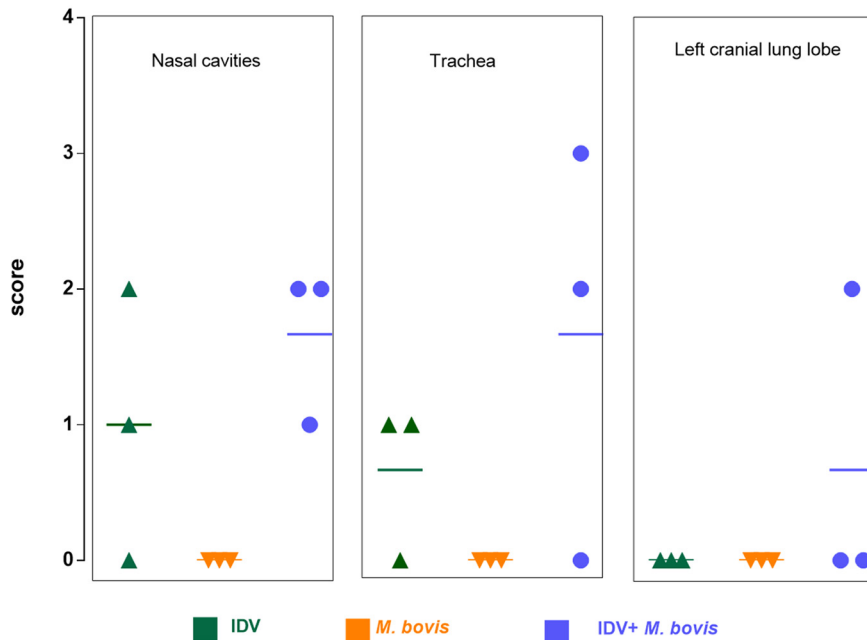


**FIG 5** The coinfection increases the microscopic lesions. Mean and individual histologic lesion scores in nasal cavity, trachea, and lung for each infected group at 6 dpi.

quantitative PCR (RT-qPCR) in deep nasal swab samples between 0 and 20 dpi (Fig. 6, top). No IDV was detected in samples from controls and *M. bovis*-infected calves. From 2 to 20 dpi, IDV was detected in IDV-infected calves, with a peak of 9.9 log<sub>10</sub> RNA copies/ml at 4 dpi. In the IDV+*M. bovis*-infected calves, most animals were positive for IDV from 2 to 10 dpi, with a peak of 10.4 log<sub>10</sub> RNA copies/ml at 4 dpi. All calves were positive for IDV from 2 to 8 dpi in the IDV group and from 2 to 6 dpi in the coinfecting group (Fig. 6, top).

*Mycoplasma bovis* was not detected in the controls, as assessed by qPCR in nasal swabs collected between 0 and 20 dpi. The *M. bovis* replication kinetics from 2 to 20 dpi showed maximum values of 5 log<sub>10</sub> (14 dpi) and 6.4 log<sub>10</sub> (4 dpi) DNA copies/ml in *M. bovis*-infected and IDV+*M. bovis*-infected calves, respectively (Fig. 6, bottom). From 14 dpi, a large majority of calves (80%) were positive for *M. bovis* in *M. bovis*- and IDV+*M. bovis*-infected calves.

Finally, in the IDV+*M. bovis*-infected group, all animals (8/8) were double positives for IDV and *M. bovis* at 4 dpi in nasal cavities.

**TABLE 1** Differential cell counts of total white cells, macrophages, neutrophils, and lymphocytes in BAL fluid samples from calves mono- or coinfecting with IDV and *M. bovis*

| Group (n = 5 calves/group) | Days postinoculation | Mean ± SEM (% unless otherwise indicated)     |             |             |             |
|----------------------------|----------------------|---|-------------|-------------|-------------|
|                            |                      | Total white cells (×10 <sup>6</sup> cells/ml) | Macrophages | Neutrophils | Lymphocytes |
| Uninfected control         | 2                    | 5.6 ± 1.6                                     | 91.1 ± 1.4  | 4.8 ± 1.7   | 0.2 ± 0.2   |
| IDV                        |                      | 5.4 ± 3.9                                     | 72.7 ± 9.9  | 12.6 ± 9.0  | 1.2 ± 1.0   |
| <i>M. bovis</i>            |                      | 8.6 ± 0.6                                     | 83.5 ± 11.1 | 8.3 ± 7.3   | 0.2 ± 0.1   |
| IDV+ <i>M. bovis</i>       | 7                    | 6.9 ± 2.2                                     | 61.9 ± 8.8  | 23.4 ± 7.8  | 0.2 ± 0.1   |
| Uninfected control         |                      | 6.4 ± 3.0                                     | 76.6 ± 8.6  | 17.2 ± 7.8  | 0.5 ± 0.5   |
| IDV                        |                      | 15.8 ± 8.0                                    | 58.9 ± 21.0 | 38.9 ± 21.0 | 0.6 ± 0.3   |
| <i>M. bovis</i>            | 14                   | 11.1 ± 4.6                                    | 51.8 ± 22.9 | 31.5 ± 14.3 | 0.5 ± 0.4   |
| IDV+ <i>M. bovis</i>       |                      | 11.1 ± 5.5                                    | 50.7 ± 13.9 | 38.3 ± 14.6 | 1.0 ± 0.6   |
| Uninfected control         |                      | 6.0 ± 2.4                                     | 70.3 ± 4.3  | 4.4 ± 1.8   | 0.7 ± 0.5   |
| IDV                        | 14                   | 13.6 ± 5.0                                    | 68.2 ± 10.8 | 7.3 ± 4.7   | 0.7 ± 0.6   |
| <i>M. bovis</i>            |                      | 11.9 ± 8.4                                    | 68.0 ± 9.8  | 13.2 ± 6.6  | 1.6 ± 0.6   |
| IDV+ <i>M. bovis</i>       |                      | 4.4 ± 2.5                                     | 58.4 ± 17.2 | 26.2 ± 16.7 | 1.4 ± 1.4   |



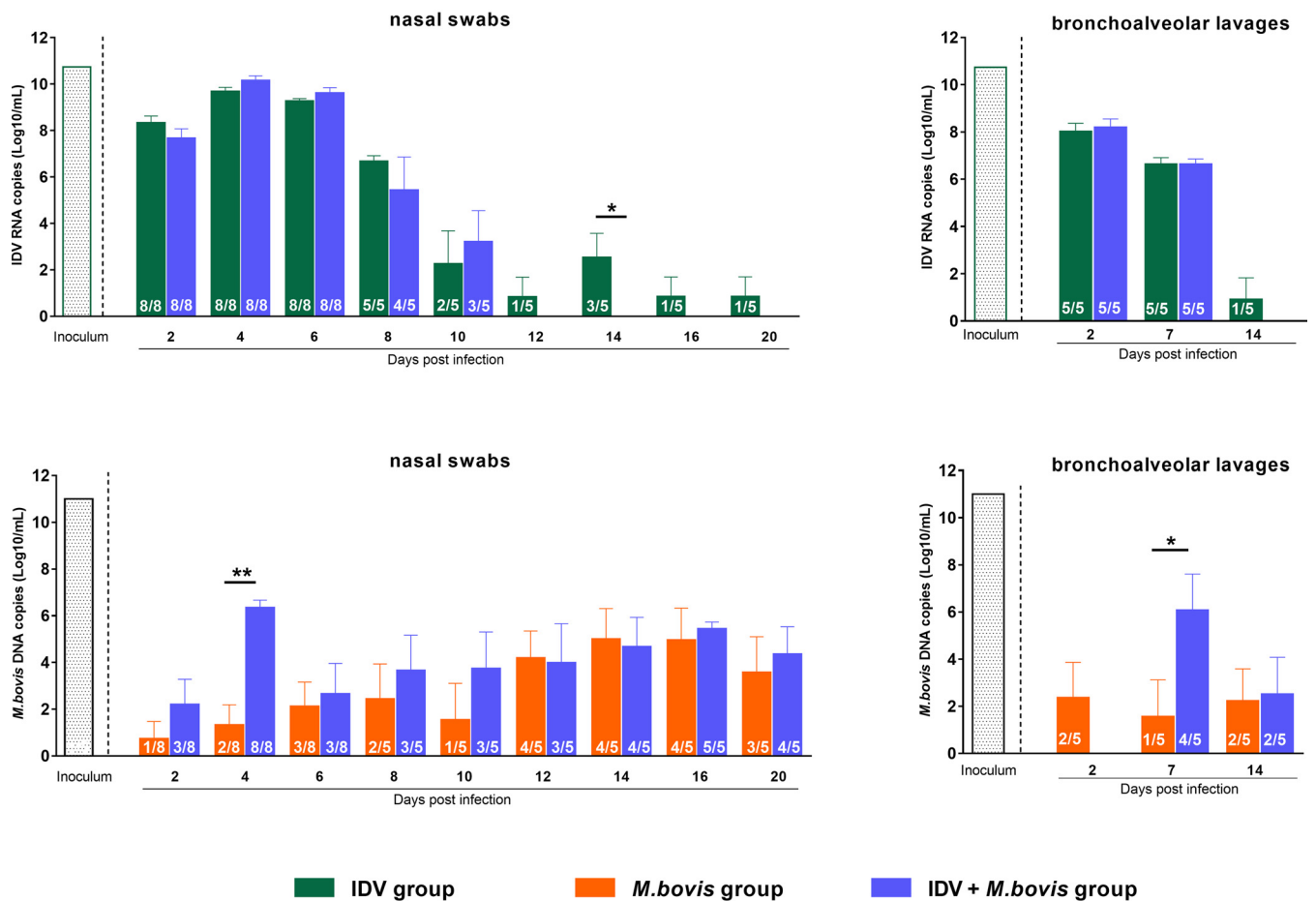


**FIG 6** IDV infection promotes *M. bovis* colonization of the upper and lower respiratory tracts. Virus titers (top) and bacterial titers (bottom) in nasal swab (left) and bronchoalveolar lavage fluid (right) samples from calves at 0 to 20 dpi and 0 to 14 dpi, respectively. Data represent the mean values  $\pm$  SEM of IDV RNA and *M. bovis* DNA copies ( $\log_{10}$ /ml) measured by RT-qPCR and qPCR, respectively. The number of positive animals/total number of animals is indicated in each bar. The titrations of the IDV ( $10.7 \log_{10}$  RNA copies/ml) and *M. bovis* ( $11 \log_{10}$  DNA copies/ml) inoculums were obtained on day zero just before they were administered to the calves by nebulization. \*,  $P \leq 0.05$ ; \*\*,  $P \leq 0.01$ .

**IDV infection promotes *M. bovis* colonization of the LRT.** We then assessed the IDV and *M. bovis* replication in BAL fluid samples (Fig. 6) and trachea and lung specimens (Table 2). No IDV was detected in control and *M. bovis*-infected calves, and no *M. bovis* was found in control and IDV-infected animals.

All IDV-infected and IDV+*M. bovis*-infected calves tested were positive for the virus in BAL fluid samples at 2 and 7 dpi (5/5) and in trachea and lungs at 6 dpi (3/3). In IDV-infected calves, the maximum viral titers were 8.5 (2 dpi), 6.8, and 6.3 (6 dpi)  $\log_{10}$  RNA copies/ml in BAL fluid samples and trachea and lung specimens, respectively. Viral titers in coinfecting animals were greater than in the IDV-infected calves, with maximum titers of 8.6 (2 dpi), 9.1, and 9.5 (6 dpi)  $\log_{10}$  RNA copies/ml in BAL fluid samples and trachea and lung specimens, respectively. Unlike in the IDV-infected calves, no virus was detected in BAL fluid samples at 14 dpi or organs at 21 dpi in the IDV+*M. bovis*-infected calves.

Considering *M. bovis*, only 40% (2/5) of the BAL fluid samples from the *M. bovis*-infected calves were positive for the bacteria from 2 to 14 dpi, with a maximum of 2.4  $\log_{10}$  DNA copies/ml at 7 dpi. In this group, *M. bovis* was exclusively detected in two of three lung samples at 6 dpi and in 4 of 5 trachea samples at 21 dpi. In comparison, most positive samples (4/5) with higher titers of bacteria (average of 6.1  $\log_{10}$  copies/ml) were observed in BAL fluid samples of the IDV+*M. bovis*-infected calves at 7 dpi. The three coinfecting animals euthanized at 6 dpi had at least 1  $\log_{10}$  *M. bovis* copies/ml more in the lung ( $n = 2/3$ ) and trachea ( $n = 3/3$ ) than the calves infected only with the bacteria.

**TABLE 2** Virus and bacteria detection in trachea and lung of calves mono- or coinfecting with IDV and *M. bovis*

| Organ   | Days postinfection | Mean copy number ( $\log_{10}$ /30 mg tissue) of RNA or DNA in indicated group (no. of positive animals/total number of animals) <sup>a</sup> : |            |                 |                           |                     |          |                 |                      |
|---------|--------------------|---|------------|-----------------|---------------------------|---------------------|----------|-----------------|----------------------|
|         |                    | IDV RNA   |            |                 |                           | <i>M. bovis</i> DNA |          |                 |                      |
|         |                    | Control   | IDV        | <i>M. bovis</i> | IDV+ <i>M. bovis</i>      | Control             | IDV      | <i>M. bovis</i> | IDV+ <i>M. bovis</i> |
| Trachea | 6                  |   | 6.81 (3/3) | ND (0/3)        | 9.09 (3/3) <sub>ABC</sub> | ND (0/3)            | ND (0/3) | ND (0/3)        | 4.79 (3/3)           |
|         | 21                 | ND (0/5)  | ND (0/5)   | ND (0/5)        | ND (0/5)                  | ND (0/5)            | ND (0/5) | 3.10 (4/5)      | 2.45 (2/5)           |
| Lung    | 6                  |   | 6.26 (3/3) | ND (0/3)        | 9.53 (3/3)                |                     | ND (0/3) | 3.06 (2/3)      | 4.39 (2/3)           |
|         | 21                 | ND (0/5)  | 4.32 (2/5) | ND (0/5)        | ND (0/5)                  | ND (0/5)            | ND (0/5) | ND (0/5)        | 3.88 (1/5)           |

<sup>a</sup>IDV RNA and *M. bovis* DNA copies were quantified by RT-qPCR and qPCR, respectively. ND, not detected. Statistical analyses were obtained with Bonferroni's multiple-comparison test by comparing each group with a *P* value of <0.01. Significant differences between IDV+*M. bovis*-infected calves and the other groups are represented by letters as follows: A, uninfected controls; B, IDV-infected calves; and C, *M. bovis*-infected calves.

The isolation of *M. bovis* was confirmed in the PCR-positive lung samples. In addition, all PCR-negative samples were also negative when isolation was attempted. These results confirm that IDV and *M. bovis* can infect the LRT of calves and that the combination of the two pathogens increases the *M. bovis* colonization of the lungs.

**Mono- and coinfections induce a humoral response against IDV in cattle.** All animals were seronegative for IDV and *M. bovis* before infections. To assess the humoral response, the antibodies against IDV from sera were first measured by hemagglutination inhibition (HI) assay with influenza virus D/bovine/France/5920/2014. Calves seroconverted against IDV from 7 dpi in both the IDV- and IDV+*M. bovis*-infected groups (Fig. 7A).

The presence of IDV-specific IgG1 and IgA was then measured in serum samples, deep nasal swab samples, and BAL fluid samples (5 calves per group) using enzyme-linked immunosorbent assay (ELISA) (Fig. 7). IDV-specific IgA and IgG1 were detected in sera of calves infected with IDV or IDV+*M. bovis* from 7 and 10 dpi, respectively (Fig. 7A). The levels of IDV-specific serum IgG1 were significantly higher in the IDV-infected calves than in the IDV+*M. bovis*-infected calves at 10 and 21 dpi, and the levels of IDV-specific serum IgA were higher in IDV+*M. bovis*-infected calves than in IDV-infected animals at 14 and 21 dpi. No IgG1 was detected in nasal swab samples (Fig. 7B) or BAL fluid samples (Fig. 7C) in IDV- and IDV+*M. bovis*-infected calves. Compared to the control calves, the mean levels of IDV-specific nasal IgA were higher in the IDV- and IDV+*M. bovis*-infected calves from 8 dpi, with maximal titers at 12 dpi. In BAL fluid samples, IDV-specific IgA was detected between 7 and 21 dpi, with maximal titers at 14 dpi, and the IgA titers were significantly higher in coinfecting calves than in IDV-infected calves at 14 and 21 dpi.

These results demonstrate that the IDV infection induces a rapid local and systemic humoral immune response.

No anti-*M. bovis* antibodies were detected by ELISA in any samples, suggesting a delayed humoral response against *Mycoplasma* infection (data not shown).

**The IDV and *M. bovis* coinfection increases the innate immune response in BAL fluid samples.** To explore the local host innate immune response, the expression levels of 52 targeted genes in BAL fluid samples were analyzed by Fluidigm PCR. These genes included those coding for pathogen recognition receptors (PRRs), cytokines, chemokines, antiviral molecules, cytokine signaling proteins, growth factors, and proteases (Table S1). No significantly different levels of expression between the four groups were observed 5 days before infection. The fold changes (FC) of gene expression levels and differentially expressed genes (DEGs) between groups at 2, 7, and 14 dpi are represented in Fig. 8.

IDV induced a quick immune response characterized by a large number of DEGs and fold changes in intensity at 2 dpi. In comparison to the gene expression in the controls, 37 of 52 genes were differentially expressed at 2 dpi, while 12 and 17 DEGs were identified at 7 and 14 dpi, respectively. Most of the genes (34/37) were overexpressed at 2 dpi. A strong antiviral response, characterized by the overexpression of IFN-

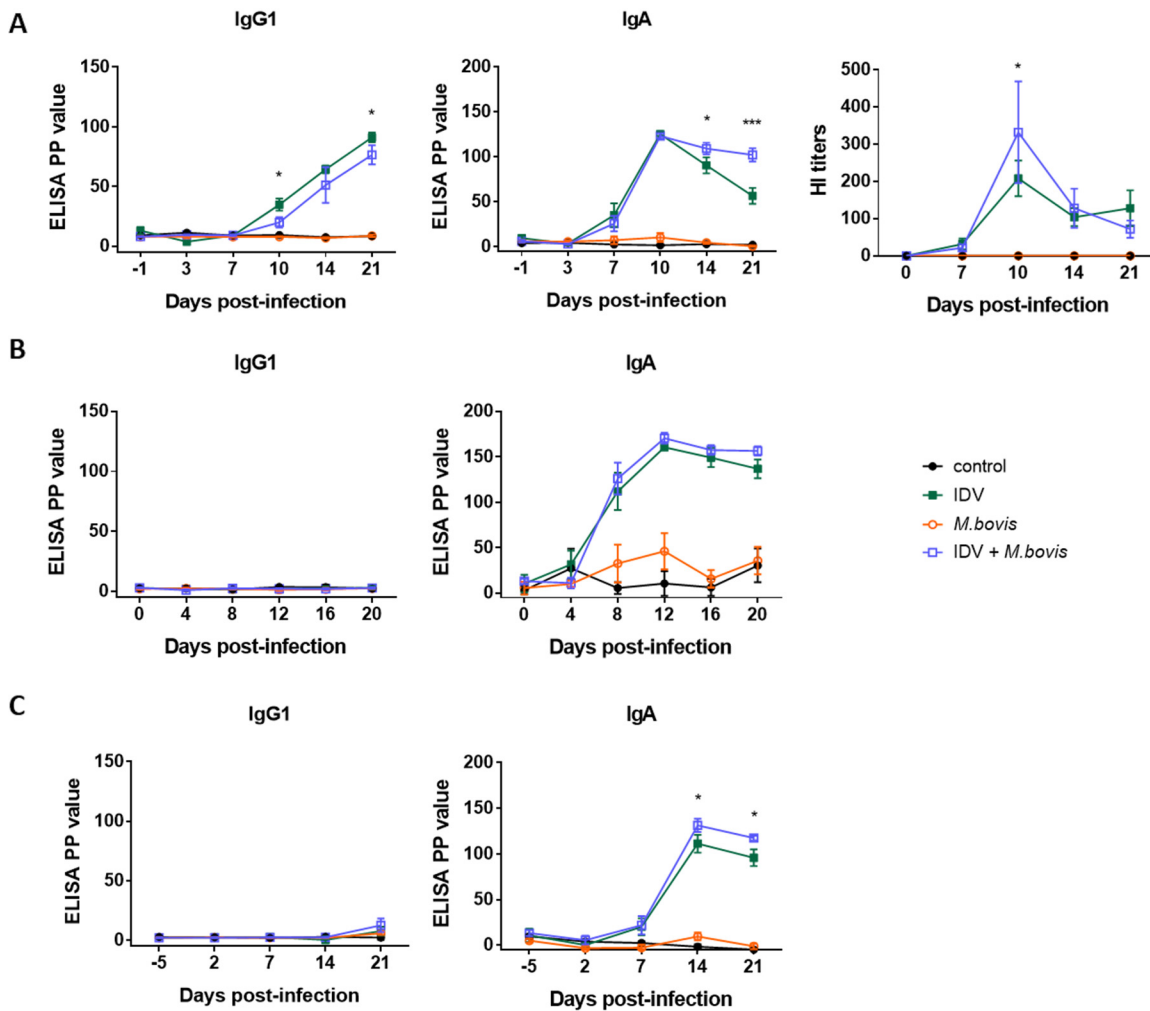


**FIG 7** IDV induced a rapid host humoral response in mono- and coinfecting calves. Total antibody, IgG1, and IgA titers from serum (A), nasal swab (B), and bronchoalveolar lavage fluid (C) samples from five calves per group were measured by HI assay with influenza virus D/bovine/France/5920/2014 for the IDV-specific antibodies and IDV-specific indirect ELISAs for IgG1 and IgA. Values are presented as means  $\pm$  SEM of the percent positivity (PP). \*,  $P \leq 0.05$  and \*\*\*,  $P \leq 0.001$  for statistically significant differences between IDV-infected and coinfecting groups using Bonferroni's multiple-comparison test.

stimulated genes (ISGs) (*IFITM1*, *IFITM3*, *ISG15*, *MX1*, and *PKR*) but a limited IFN- $\beta$  response (*IFN- $\beta$ 1*) was identified. Moreover, the high levels of chemokines (*CCL2*, *CCL3*, *CCL4*, *CCL8*, *CXCL2*, and *IL-8*), interleukins (*IL-1 $\alpha$* , *IL-1 $\beta$* , *IL-6*, *IL-10*, *IL-12 $\beta$* , and *IL-15*), and *TNF- $\alpha$*  demonstrated the setting up of a proinflammatory state with a potential to recruit, activate and induce cellular proliferation of leukocytes in the lung. Lymphocyte activation was confirmed by the overexpression of *IFN- $\gamma$* , mainly at 7 dpi. The viral infection led to significant overexpression of PRR genes, mainly *DDX58*, *IFIH1*, *TLR2*, and *TLR4*. In addition, a limited increase of *TLR3* and *TLR7* was found at 2 dpi. Some signaling molecules (*IRF1*, *MAVS*, *MyD88*, *NF- $\kappa$ B*, *SOCS1*, *SOCS3*, and *STAT1*) and growth factors (*TGF $\alpha$*  and *VEGFA*) were also significantly dysregulated during IDV infection.

Considering *M. bovis* infection, we found a late and low local host response with a limited dysregulation of targeted genes. In comparison to the gene expression in the controls, only four genes (*DDX58*, *IFN- $\beta$ 1*, *IFNGR2*, and *MAVS*) were statistically underexpressed after 2 dpi with *M. bovis*. Most DEGs were identified at 7 dpi, with a total of 17 genes overexpressed. These genes play roles in the proinflammatory response and white cell recruitment (*CCL3*, *IL-1 $\alpha$* , *IL-1 $\beta$* , *I-L8*, *IL-10*, *IL-15*, and *TNF- $\alpha$* ) and also in antiviral and signaling pathways (*IFIH1*, *IFITM3*, *IFNGR2*, *MX1*, *MyD88*, *SOCS3*, *TLR2*, and *TLR4*).

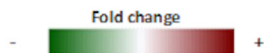
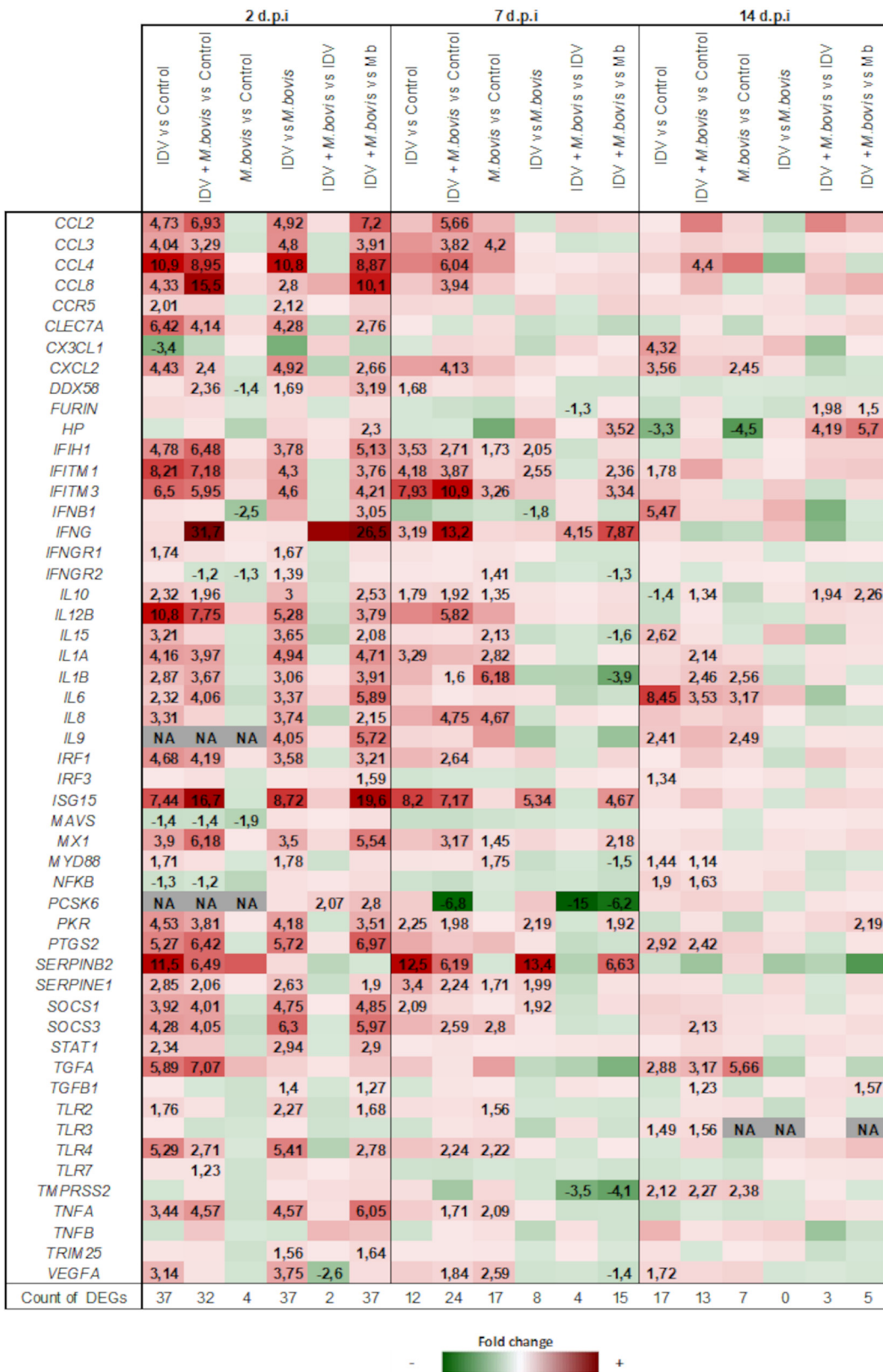


**FIG 8** The coinfection increased the innate immune response in BAL fluid samples. Fold changes in the mRNA expression (Fluidigm) of 52 bovine genes from BAL fluid samples of mono- or coinfecting calves. The fold changes in mRNA expression were calculated for pairs of groups at 2, 7, and 14 dpi. Positive fold changes are colored in red, and negative fold changes in green. The fold change values of differentially expressed genes (DEGs) with a significant difference ( $P < 0.05$ ) are presented.



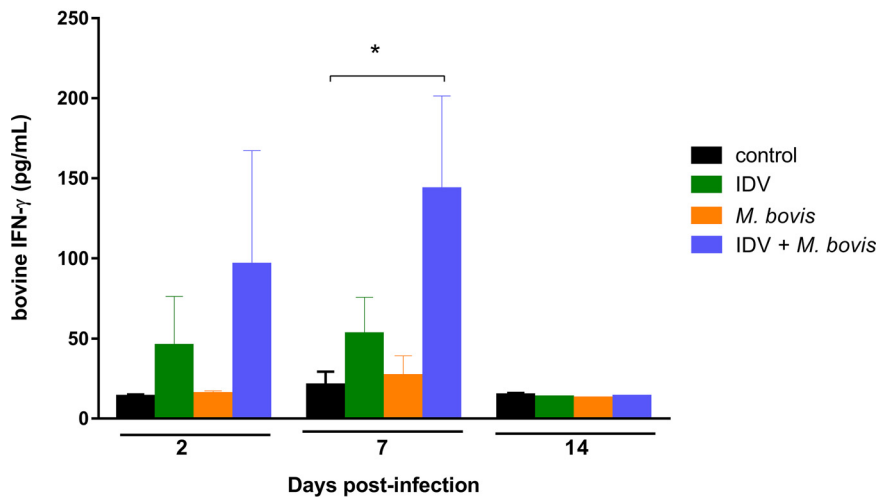


**FIG 9** The coinfection increased the IFN- $\gamma$  synthesis in BAL fluid samples. Bovine IFN- $\gamma$  levels were measured in BAL fluid samples by sandwich ELISA. Data are presented as mean values  $\pm$  SEM for the cytokine concentrations (pg/ml). \*,  $P \leq 0.05$  for statistical difference between control and coinfecting groups using Bonferroni's multiple-comparison test.

The comparison between gene expression in IDV- and *M. bovis*-infected calves confirms the induction of a faster and stronger host response by IDV.

A rapid and high response was finally observed in the coinfecting calves. In comparison to the gene expression in the controls, 32 DEGs were found, with 29 overexpressed and 3 underexpressed at 2 dpi. Compared to the gene expression in the controls, the coinfection led to 24 and 13 DEGs at 7 and 14 dpi, respectively. In addition to the DEGs found in the IDV-infected group, the coinfection induced significant overexpression of *CCL2*, *CCL3*, *CCL4*, *CCL8*, *CXCL2*, *IL-1 $\beta$* , *IL-8*, *IL-12 $\beta$* , *IRF1*, *MX1*, *SOCS3*, *TLR4*, *TNF- $\alpha$* , and *VEGFA* and downregulation of *PCSK6* at 7 dpi. Nevertheless, compared to the gene expression in the IDV-infected calves, only the overexpression of IFN- $\gamma$  and downregulation of *FURIN*, *PCSK6*, and *TMPRSS2* were statistically different in the coinfecting versus the IDV mono-infected calves at 7 dpi. Many differences were identified between the coinfecting and *M. bovis*-infected calves, particularly at 2 and 7 dpi. Finally, only the overexpression of IFN- $\gamma$  and the downregulation of *PCSK6* and *TMPRSS2* were statistically different when the coinfecting group was compared to the IDV- and *M. bovis*-mono-infected groups at 7 dpi (Fig. 8).

To confirm the overexpression of IFN- $\gamma$ , we analyzed the production of this cytokine by ELISA. We found increased production of the IFN- $\gamma$  cytokine in BAL fluid samples of IDV-infected and coinfecting groups at 2 and 7 dpi (Fig. 9). Compared to the IFN- $\gamma$  production in the control group, the IFN- $\gamma$  production of the IDV group was increased on average by 3.3- and 2.5-fold at 2 and 7 dpi, respectively. The highest overproduction was observed in the coinfecting group, with 7.1- and 6.9-fold increases at 2 and 7 dpi, respectively. No real differences in cytokine production were measured between the control and the *M. bovis*-infected group. At 14 dpi, the IFN- $\gamma$  protein levels were similar in all groups.

## DISCUSSION

In agreement with our previous study, where the same IDV challenge strain, inoculation dose, and route were used (18), and other similar studies (17, 26), we confirmed that IDV alone causes moderate respiratory clinical signs. Furthermore, the replication kinetics, the nasal, tracheal, and lung lesions, and the short IgG response were all similar to our previous results (18). We also used this experiment to further investigate the intestinal tropism of influenza virus D/bovine/France/5920/2014 previously described by Oliva et al. (28) in a mouse model. We were able to detect IDV by RT-qPCR in fecal

swab samples (2/8 calves) at 5 dpi and in the jejunum (1/3 calves) at 6 dpi (data not shown), corresponding to the viral replication peak in the respiratory tract. Intestinal tropism and infectivity must be confirmed by immunohistochemistry and isolation studies, but these preliminary results raise the question of possible IDV contamination through the digestive tract, in addition to the aerosol transmission previously described (18).

In this study, we chose to do a coinfection at the same time because it better mimics the field conditions of BRD, in which veal calves from many herds are grouped for a short time, allowing rapid and concurrent contaminations by pathogens. Three- to 8-week-old calves were used, as in other studies where clinical signs and lesions typical of *M. bovis* pneumonia were successfully reproduced (29–32). Using the recently isolated French *M. bovis* strain RM16 and a challenge by nebulization, we were able to induce cough, increased nasal discharge, fever, and tachypnea, especially from 8 to 18 dpi. These observations suggest that *M. bovis* has a particular tropism and pathogenicity for the URT, mainly in the nasal cavity, trachea, and primary bronchi, as previously described (29–32). This is correlated with the high bacterial loads found in the nasal cavities and the trachea. However, we were not able to reproduce typical clinical signs of severe bronchopneumonia in the *M. bovis*-infected calves, nor to observe macroscopic and microscopic lesions at 6 or 21 dpi in lung tissues. Furthermore, the *M. bovis* DNA loads detected in the BAL fluid samples at 2 and 7 dpi were low, which could explain the absence of gene transcriptional activation in BAL fluid samples at 2 dpi and the overexpression at 7 dpi of only a few genes (*TLR2*, *TLR4*, *IL-1 $\alpha$* , *IL-1 $\beta$* , *IL-8*, *TNF- $\alpha$* , and *CCL3*), contrary to what was detected in calves infected with IDV or IDV+*M. bovis*. Altogether, these data could suggest an effective and rapid pulmonary bacterial clearance and/or a limited tropism and/or pathogenicity of *M. bovis* strain RM16 to the lung parenchyma under our experimental conditions. On the other hand, since the clinical signs were mainly observed from 8 to 18 dpi, it is possible that we sampled tissues too early and missed lesions that would have correlated with the clinical peak at 13 dpi. We observed histopathological lung lesions in one *M. bovis*-infected calf at 21 dpi, as observed in other publications when calves were necropsied at 21 to 60 dpi (29–32). Further kinetic analyses will be necessary to properly characterize the role of *M. bovis* strain RM16 in BRD of calves.

The main result here is the fact that, when associated, IDV and *M. bovis* enhanced respiratory clinical signs and shortened the incubation period. Compared to the clinical signs of the *M. bovis*-infected calves, those of the coinfecting animals were similar yet more severe, suggesting that IDV facilitates *M. bovis* disease. We also detected more respiratory signs of bronchopneumonia in the coinfecting calves than in the IDV-infected calves, suggesting that each pathogen may potentiate the clinical effect of the other. The enhanced disease during coinfection did not seem to be statistically correlated with differences of IDV and *M. bovis* replication in nasal secretions, despite slightly higher bacterial loads in nasal swab samples of the coinfecting group between 2 and 10 dpi (statistically different at 4 dpi). On the other hand, the genomic DNA loads of *M. bovis* were significantly higher in BAL fluid samples at 7 dpi and in the trachea at 6 dpi when calves were coinfecting with IDV, suggesting that IDV facilitates the replication of *M. bovis* in the LRT during the first days of infection. This may explain the macroscopic and histologic observations showing that the coinfection promotes not only tracheobronchitis but also interstitial bronchopneumonia with fibrinopurulent exudate and lung atelectasis. This also correlates with the observation of more severe clinical signs of LRT infection between 3 and 8 dpi for the coinfecting calves than for mono-infected calves. Two studies of coinfections in calves were published using IDV or *M. bovis*, but they were performed in a sequential mode, with a viral infection first, followed by a bacterial infection. The first study showed that bovine herpesvirus type 1 facilitates the pathology induced by *M. bovis* in cattle, including chronic pneumonia and polyarthritis syndrome in calves (27). In the second study, Zhang et al. failed to exacerbate the respiratory signs in calves when they performed an IDV infection followed 5 days later by an *M. haemolytica* infection

(26). Several factors, such as the IDV strain, different bacterial species, or coinfection versus temporally separated infection may explain differences in our study. In the study of Zhang et al., the low pathogenic challenge with *M. haemolytica*, as observed in mono-infected calves, may also explain the absence of enhanced symptomatology in coinfecting animals (26).

When we analyzed the transcriptional response of white cell genes in BAL fluid samples at 2 dpi, both IDV and IDV+*M. bovis* infections had induced rapid differential expression of a high number of genes (37/52 and 32/52 genes, respectively) compared to the gene expression in the control calves. These genes are involved in the innate immune response and especially in the interferon type I signaling and the proinflammatory chemokine and cytokine responses. The overexpression of *TNF- $\alpha$* , *IL-1 $\alpha$* , *IL-1 $\beta$* , *CCL2*, *CCL4*, *IL-8*, and *CX3CL1* mRNAs from BAL fluid samples of IDV-infected calves at 2 and 7 dpi correlates with the increases of the total leukocyte counts in the BAL fluid samples at 7 and 14 dpi, partly due to the increase of macrophages, monocytes, and neutrophils. At 7 dpi, the high levels of lymphocytes and *ifn- $\gamma$*  transcription suggest macrophage and dendritic cell activation, as highlighted by the overexpression of proinflammatory *IL-1 $\alpha$*  and *IL-1 $\beta$*  cytokines during IDV infection. At the same time, IDV infection also induced neutrophil diapedesis in the lungs, as determined by the high white cell counts in BAL fluid samples and corresponding to the overexpression of *CCL3*, *CXCL2*, and *IL-8* genes. In the mouse model, primary influenza A virus (IAV) infection was shown to increase macrophages and neutrophils in the airway lumen but was associated with dysfunctions (like phagocytosis) that prevented bacterial clearance and promoted a secondary bacterial infection (33). Conversely, IAV infection was also shown to induce alveolar macrophage depletion, increasing the susceptibility to secondary infection (21, 34, 35). In agreement with our cattle study, Skelton et al. (36) recently showed that intratracheal IDV infection in mice increased the recruitment of neutrophils and lymphocytes and did not deplete macrophage counts in the lungs of mice euthanized at 7 dpi. On the other hand, no clinical signs were observed in another study after IDV infection alone in mice (28). This contrasts with the natural model of the calf where respiratory clinical signs were clearly described (17, 18).

Although not statistically different, coinfection with IDV and *M. bovis* induced a global RNA expression pattern with higher fold changes than IDV alone that suggested that it favors the transcription of genes involved in the innate and adaptive immune responses. At 7 dpi, 22 genes in the coinfecting calves were statistically overexpressed in comparison with their expression in the control animals, which was not the case for the IDV-infected calves. This coincides with higher replication of *M. bovis* in the BAL fluid samples and lung histopathological lesions in the coinfecting group, suggesting that the extended innate immune response against IDV may participate in the severity of *M. bovis* pathogenicity. Surprisingly, and despite chemokine mRNA overexpression in the coinfecting group (especially for *CCL2*, *CCL8*, *ISG15*, and *IFN- $\gamma$*  genes), the monocyte/macrophage rate increased only slightly at 7 dpi. At 14 dpi, there even seemed to be a depletion of monocytes/macrophages in the BAL fluid samples in this group. We do not know if the presence of *M. bovis* may limit the recruitment or may contribute to the destruction of macrophages in the airway lumen, thus facilitating the severity of the disease. In addition, even if all three types of infections induced neutrophil diapedesis in calves, the neutrophil fraction in the coinfecting animals at 2 and 7 dpi (23.4 and 38.3%, respectively) played an important contribution in increasing the number of leukocytes in the BAL fluid samples. This is consistent with previous studies where IAV superinfection with *Staphylococcus aureus* or *Streptococcus pneumoniae* in mice 3 to 6 days later resulted in enhanced neutrophilic inflammation in the lungs (37, 38). On the other hand, similar transcription rates were observed at 2 dpi between calves of the two groups for the *CCL3*, *CXCL2*, and *IL-8* genes (37, 38). We do not know if these earlier and higher numbers of neutrophils in the BAL fluid samples of the IDV+*M. bovis*-infected calves at 2 dpi contribute to the rapid host response or facilitate the emergence of clinical signs. As we performed coinfections and not superinfections,

comparisons with previous publications of IDV superinfections in calves or mice are difficult. Using IDV, Skelton et al. showed that intratracheal IDV inoculation in mice protected against a secondary *Staphylococcus aureus* infection (36), suggesting that macrophages may be involved in mediating protection from secondary bacterial challenge by neutrophils and lymphocytes. In addition to differences in infection kinetics, the types of bacteria used in each challenge may also explain the exacerbation of the respiratory disease we observed for IDV coinfection with *M. bovis* in calves. In the mouse model, Skelton et al. suggested that the IFN- $\beta$  response after IDV infection prevented susceptibility to secondary bacterial infection (36). Conversely, in the IAV-*S. aureus* superinfection model, influenza virus-induced type I IFNs have been shown to inhibit IL-23 production, which is required for the generation of type 17 immunity and for effective clearance of secondary *S. aureus* pneumonia (37). In calves, our results support that IDV alone or in association with *M. bovis* induced at 2 and 7 dpi a similar overexpression of ISG mRNAs (mainly *MX1*, *PKR*, *IFIH1*, *IFITM1*, *IFITM3*, and *ISG15*), confirming the activation of the IFN-I pathway by the virus but without statistical differences between the two groups. Consequently, the overexpression of IFN-I-related genes probably does not explain disease differences.

Finally, when we performed direct comparisons between infected groups, almost the same genes were differentially expressed at 2 dpi when *M. bovis* infection was compared to IDV or IDV+*M. bovis* infections. At 7 dpi, differences were more numerous between the *M. bovis* and IDV+*M. bovis* groups, suggesting a cooperative effect of these two pathogens. When the coinfecting group was compared to the two mono-infected groups at 7 dpi, only three genes were statistically differentially expressed: the *IFN- $\gamma$*  gene with relative overexpression and *PCSK-6* and *TMPRSS2* with relatively lower expression in coinfecting animals. In particular, the *IFN- $\gamma$*  gene was shown to be the most statistically overexpressed gene very quickly after infection at 2 dpi (FC of 31.7) and at least until 7 dpi (FC of 13.2). This was confirmed by higher production of IFN- $\gamma$  protein in the coinfecting group than in the other groups. This correlates with the high level of lymphocytes in BAL fluid samples of coinfecting calves mainly at 7 dpi. It could be speculated that this cytokine, mainly produced by natural killer (NK) cells, T helper 1 (Th1) cells, and cytotoxic T lymphocytes (CTL), is directly involved in the enhanced disease of coinfecting animals. Indeed, previous publications have reported that mice deficient in IFN- $\gamma$ -mediated signaling were protected from IAV-*S. aureus* superinfection (37) and that depletion or dysfunction of alveolar macrophages during IAV infection in mice depends on the level of IFN- $\gamma$  production and the mouse strain (33, 39), confirming the importance of this cytokine in bacterial phagocytosis by the macrophages.

As mainly observed in BAL fluid samples and serum samples but also in nasal swab samples, the IgA levels were higher in coinfecting than in IDV-infected calves at 14 and 21 dpi. This piece of information correlates with the increase of lymphocyte counts in BAL fluid samples from 7 dpi in this group. As previously described for other viruses (40–42), we can postulate that the elevated IgA levels in coinfecting calves may contribute to the earlier reduction of IDV loads in the respiratory tract of these animals.

Dysregulations of other genes known to play a role in influenza pathogenesis were detected. *PCSK-6* and *TMPRSS2* encode serine endoproteases (PACE4 and TMPRSS2) that process proproteins trafficking through regulated or constitutive branches of the secretory pathway. While the role of PACE4 in the proteolytic activation of the hemagglutinin of IAV is still being discussed, the TMPRSS2 protein was recently shown to be essential for the spread and pathogenesis of H1N1, H3N2, and H7N9 IAV strains, to facilitate the entry into host cells by proteolytic cleavage and activation of the hemagglutinin (HA) protein (43–45). This protein is highly expressed in the respiratory tract, especially in the lungs (46). Our study clearly shows that the transcription of these two genes is repressed at 7 dpi in the coinfecting calves. Interestingly, the *furin* gene also seemed underexpressed when coinfection was compared to IDV mono-infection at this time point. The reason why these genes, which are known to facilitate influenza virus spread, are underexpressed in the coinfecting group remains to be elucidated, but their



downregulation at 2 and 7 dpi precedes the decrease of IDV RNA loads in BAL fluid samples and lung tissues at 14 and 21 dpi, respectively. This piece of information confirms the importance of exploring the capacity of these proteases to activate the IDV hemagglutinin-esterase-fusion (HEF) glycoprotein, as suggested by Su et al. (47).

To conclude, the results of the present study show that IDV and *M. bovis* coinfection in calves is associated with extension of the distribution of *M. bovis* in the lung, exacerbated respiratory pathogenicity, and a strong and prolonged transcriptomic innate immune response in the LRT, especially highlighted by IFN- $\gamma$  overexpression. Further studies are being carried out to decipher the cellular mechanisms involved.

## MATERIALS AND METHODS

**Virus and bacteria.** The influenza D virus strain D/bovine/France/5920/2014 was isolated from the lung of a dead calf with clinical signs of BRD (9). The virus was propagated on human rectal tumor cells (ATCC CRL-11663) in Dulbecco's modified Eagle's medium (DMEM; Dutscher, France) supplemented with 1  $\mu$ g/ml TPCK (tosylsulfonyl phenylalanyl chloromethyl ketone)-trypsin (Thermo Fisher Scientific, MA, USA) at 37°C, 5% CO<sub>2</sub> for 5 days. Viral titer was determined on swine testis cells (ATCC CRL-1746) using the 50% tissue culture infective dose (TCID<sub>50</sub>) method as previously described (17).

*M. bovis* strain RM16 was isolated in 2016 in France from a pool of transtracheal aspiration samples from 3 heifers with clinical signs of respiratory infection (48). Mycoplasma cells were grown in SP4 medium (49) supplemented with cephalixin (500  $\mu$ g/ml). After 24 to 36 h of incubation at 37°C, mycoplasma cultures were stored at -80°C. Mycoplasma titers were determined by serial dilutions in Dulbecco's phosphate-buffered saline (PBS; Invitrogen) supplemented with 1% heat-inactivated horse serum (Invitrogen). Dilutions were spotted (10  $\mu$ l) onto solid SP4 medium, and CFU were counted after 2 to 5 days of incubation at 37°C. For animal inoculations, mycoplasma cells were washed twice in DMEM by 20 min of centrifugation at 9,000  $\times$  g and kept on ice. Prior to inoculation, 10<sup>10</sup> CFU were diluted in 10 ml DMEM.

**Safety and ethics.** The animal experiment was performed in biosafety level 3 facilities at the Research Platform for Infectious Disease (PFIE, National Institute for Agronomic Research, INRAE, Nouzilly, France) in accordance with humane standards of animal care (50) and under a national ethical agreement (number APAFIS 16364-2018080211232403; French Ministry of Agriculture, Ethics Committee no. 019).

**Calves and experimental infections.** Twenty-nine Normand and Holstein calves, born at the experimental farm of INRAE-Le Pin (Exmes, France), were used in this study. At birth, the calves received anti-IDV- and anti-*M. bovis*-specific-antibody-free colostrum (SLU, Sweden). They were transferred to the PFIE at the age of 3 to 6 days. The animals were fed twice a day with commercial reconstituted milk and pellets during 3 to 8 weeks before inoculation. Before challenge, all calves were confirmed to be negative for the presence of *M. haemolytica*, *P. multocida*, *M. bovis*, *H. somni*, BCoV, IDV, BRSV, and BPIV-3 pathogens in nasal swab samples by real-time PCR (Bio-T respiratory qPCR kits; BioSella, France). The absence of BVDV was confirmed by analyzing the nonstructural protein 3 (NS3) antigen by ELISA in serum (SERELISA BVDV-BD; Synbiotics, Lyon, France). Before the challenge, calves were confirmed negative for *M. bovis*- and IDV-specific antibodies by ELISA (Bio K 302; BioX diagnostics, Belgium) and hemagglutination inhibition (HI) assay, respectively. The 29 calves were split into the following four groups (the age distribution was harmonized) in separate rooms: control (uninfected) ( $n = 5$ ), IDV infected ( $n = 8$ ), *M. bovis* infected ( $n = 8$ ) and IDV+*M. bovis* infected ( $n = 8$ ) (Fig. 1). Infected calves were inoculated at day zero by nebulization as previously described with 10<sup>7</sup> TCID<sub>50</sub> of influenza virus D/bovine/France/5920/2014 and/or 10<sup>10</sup> CFU of *M. bovis* RM16 in 10 ml of DMEM (18, 30). Control animals were inoculated with 10 ml of DMEM.

**Clinical observation.** Calves were examined by the same veterinarian twice a day from 3 days before infection to 21 dpi for their general state, decreased appetite during feeding, rectal temperature, nasal discharge, coughing, abnormal breathing, respiratory rate, and abnormal lung sounds. Clinical scores were assessed for each calf as previously described (3) with slight modifications. Briefly, scores for rectal temperatures ( $T$ ) were 0 ( $T < 39^\circ\text{C}$ ), 1 ( $39.1^\circ\text{C} < T < 40^\circ\text{C}$ ), 2 ( $40.1^\circ\text{C} < T < 41^\circ\text{C}$ ), or 3 ( $T > 41^\circ\text{C}$ ); scores for respiratory rates per minute (RR/min) were 0 ( $\text{RR} < 35$ ), 1 ( $35 < \text{RR} < 40$ ), 2 ( $41 < \text{RR} < 60$ ), 3 ( $61 < \text{RR} < 80$ ), or 4 ( $\text{RR} > 80$ ); scores of 0 (normal), 1 (mild), or 2 (severe) were given for nasal discharge and general state; and dyspnea (absent, weak, moderate, or high) and appetite (drop in milk consumption of 0%, <30%, 30 to 60%, or > 60%) were scored from 0 to 3. Finally, two scores were assigned for coughing according to frequency (0, absent; 1, occasional cough; or 2, frequent cough) and severity (0, absent; 1, moderate; or 2, strong cough with violent efforts). Daily individual accumulated scores were calculated for each calf by adding the score of each parameter. Finally, the mean ACS was calculated for each group as the mean of the individual areas under daily clinical scores using the trapezoid method (GraphPad, La Jolla, CA USA).

**Gross lesions and histopathology.** Three animals per infected group (randomly selected before the challenge) were euthanized at 6 dpi to assess the early lesions. The remaining calves (five per group) were euthanized at 21 dpi. Euthanasia was carried out by intravenous injection of pentobarbital sodium (Dolethal, 180 mg per kg of body weight; Vetoquinol, France) followed by complete exsanguination. The tissue samples collected were as follows: right and left cranial, middle, and right and left caudal lobes of the lungs, nasal and tracheal mucosa, tonsils, lymph nodes (mediastinal, tracheobronchial, and

mesenteric), olfactory bulb, kidney, spleen, liver, and intestine (duodenum, jejunum, ileum, and colon). Every tissue and organ sample was divided into three parts, one in 10% buffered formalin for histology and two stored at  $-80^{\circ}\text{C}$  for RNA and DNA extractions. Examination and scoring of gross lesions, tissue sampling, and histopathology were carried out as previously described (18). For histopathology, a pathologist described and scored the severity of microscopic lesions in slides of lung and respiratory lymph node samples as either light (3 or fewer small lesion foci in one section, score of 1), moderate ( $>3$  small lesion foci per section, score of 2), or marked (diffuse lesions in the section, score of 3).

**Sample collection and preparation.** Nasal swabs were collected daily from 3 days before infection to 21 dpi in 1 ml of PBS and stored at  $-80^{\circ}\text{C}$  until extraction of nucleic acids. To quantify mucosal IDV-specific IgG1 and IgG2, sanitary tampons were introduced every 4 days into the left nasal cavity of each calf for 10 min during milk meals. The tampons were removed and pressed to obtain mucosal fluids (between 2 to 5 ml), which were stored at  $-80^{\circ}\text{C}$  until ELISAs could be performed. Five days before infection and 2, 7, and 14 dpi, BAL fluid samples were obtained from the same 5 calves per group. Briefly, local anesthesia of the nasal cavities was carried out using a nasal spray containing 2% xylocaine. Five minutes later, the calf was restrained and a first sterile tube (food-grade silicone, 35 cm long, with external and internal diameters of 12 and 8 mm, respectively) covered with anesthetic ointment (2% xylocaine) at the end was introduced into the right nasal cavity and then into the proximal trachea. A second tube (food-grade silicone [Vitryl], 130 cm long, with external and internal diameters of 6 and 4 mm, respectively) was introduced into the first tube and pushed over 1 meter deep until meeting resistance inside the narrow bronchial lumen. Quickly, 100 ml of sterile isotonic sodium chloride solution was injected down the BAL tube using a sterile syringe and immediately aspirated. Between 50 and 80 ml was recovered. The supernatants and white cells from BAL fluid samples (obtained after centrifugation of 30 ml at  $300 \times g$  for 20 min) were stored at  $-80^{\circ}\text{C}$ . Fecal swab samples were collected the day before infection and at 2, 5, 8, 11, and 14 dpi in 2 ml of PBS and stored at  $-80^{\circ}\text{C}$ . Blood samples were collected 1 day before infection and at 3, 7, 10, 14, and 21 dpi. Serum was extracted from the blood by centrifugation ( $800 \times g$  for 20 min) and was stored at  $-20^{\circ}\text{C}$ .

**BAL fluid samples and white cell populations.** The cellular composition in BAL fluid samples was determined using the Cytospin 3 system (Thermo Fisher Scientific, MA, USA) and MGG staining. Briefly, 10 ml of fresh BAL fluid was centrifuged at  $300 \times g$  for 20 min. Cell pellets were resuspended in 500  $\mu\text{l}$  of PBS. The Cytofunnels mounted with slides were loaded with 125- $\mu\text{l}$  amounts of resuspended cells. After centrifugation at  $300 \times g$  for 10 min, the slides were stained with May-Grünwald and Giemsa solutions (RAL Diagnostic, France). A minimum of 100 cells was observed under an optical microscope to identify the white cell populations in BAL fluid samples.

**RNA and DNA extractions.** Viral RNA and bacterial DNA were extracted from 170- $\mu\text{l}$  amounts of nasal swab, raw BAL fluid, and fecal swab samples using the NucleoMag pathogen kit (Macherey-Nagel, Germany) on the KingFisher Flex purification system (Thermo Fisher Scientific, MA, USA) according to the manufacturer's instructions. Total RNA was extracted from pelleted cells of BAL fluid samples with the NucleoMag RNA kit (Macherey-Nagel, Germany) on the KingFisher Flex purification system (Thermo Fisher Scientific, MA, USA). Extraction of viral RNA and bacterial DNA from tissues (30-mg amounts of nasal turbinate, trachea, and lung lobe samples) were obtained by lysis in Precellys lysing kit tubes (catalog number P000912-LYSKO-A; Bertin Technologies, France) with 500  $\mu\text{l}$  of Opti-MEM on a Precellys system (Bertin Technologies, France). Nucleic acids were then extracted using the NucleoSpin RNA virus kit (Macherey-Nagel, Germany).

**IDV and *M. bovis* quantification.** Influenza D virus was quantified in nasal swab, BAL fluid, and tissue samples using a one-step RT-qPCR as previously described (10). Briefly, the viral polymerase basic 1 (PB1) gene was amplified with specific primers and quantified by using a specific probe and the QuantiNova probe RT-PCR kit (Qiagen, Germany) on a LightCycler 96 real-time PCR system (Roche, Switzerland). Viral copy numbers in samples were determined by using a standard plasmid containing the PB1 product of influenza virus D/bovine/France/5920/2014 (18). For quantification of *M. bovis* genomic DNA copy numbers in nasal swab, BAL fluid, and tissue samples, qPCR was performed with specific primers, probe, and specific standard using the Bio-T *Mycoplasma bovis* PCR kit (Biossellal, France) on the LightCycler 96 real-time PCR system (Roche, Switzerland) according to the manufacturer's instructions.

**Host humoral response.** The IDV-specific antibody titers in animal sera were determined by HI assay as previously described (18). The IDV-specific IgG1 and IgA raised against IDV in BAL fluid, nasal swab, and serum samples were assessed using either indirect or capture ELISAs. The indirect ELISA was as previously described (18, 51), and the capture ELISA was designed according to Uttenthal et al. (52). ELISA plates (MaxiSorp; Nunc, Denmark) were coated for 18 h at  $4^{\circ}\text{C}$  with 100 ng mouse anti-bovine IgA (interleukin A71 [IL-A71], catalog number MCA2438; Bio-Rad Laboratories, Inc., Solna, Sweden) per well in coating buffer containing 0.05 M Na-carbonate bicarbonate, pH 9.6. The wells were thereafter blocked for 1 h at  $25^{\circ}\text{C}$  with PBS containing 2% (wt/vol) bovine serum albumin, before the addition of (i) samples diluted 1:25 (nasal secretions) or 1:10 (BAL fluid), (ii) IDV antigen or cell control (cell culture medium from CRL1756 cells infected with influenza virus D/bovine/France/5920/2014 or similar uninfected cells), (iii) mouse anti-IDV antibodies (monoclonal antibody [MAb] 4F1) produced and characterized as described previously (31), or (iv) rat anti-mouse IgG1 conjugated with horseradish peroxidase (HRP) (clone LO-MG1-2, catalog number MCA336P; Bio-Rad), TMB (3,3',5,5'-tetramethylbenzidine) substrate, and  $\text{H}_2\text{O}_2$ . Each antibody or antigen solution was added in a volume of 100  $\mu\text{l}$  per well and incubated for 1 h at  $37^{\circ}\text{C}$ , prior to three washes with 0.05% PBS-Tween 20 solution. To analyze the IDV-specific IgG1 and IgA titers, the optical density (OD) was measured at 450 nm on a microplate reader. Corrected OD (COD) values were calculated by subtracting the OD values of wells containing control antigen from

those of wells containing IDV antigen. Data were expressed as percent positivity (PP) values, corresponding to the COD of the sample divided by the COD of the positive control. Detection of antibodies against *M. bovis* was performed with a commercial ID Screen *Mycoplasma bovis* indirect ELISA kit (Innovative Diagnostics, France). The antibody titers were calculated according to the manufacturer's guidelines.

**Transcriptomic analyses from BAL fluid samples.** Host gene expression levels in the BAL fluid samples collected 5 days before infection and at 2, 7, and 14 dpi were compared. Briefly, cDNA synthesis was performed from 100 ng of RNA from BAL fluid samples by using random hexamer primers and RevertAid reverse transcriptase (Thermo Fisher Scientific, MA, USA) according to the manufacturer's instructions. The sets of primers were previously selected (17), and new primer pairs were designed from bovine RNA sequences. Gene primers were preferentially designed between two exons by using Primer3 software and validated by using an RT-qPCR protocol on the LightCycler 96 real-time PCR system (Roche, Switzerland). The primer pairs and targeted genes are listed in Table S1. A total of 76 bovine genes playing roles in the antiviral response, inflammatory response, chemotaxis, and/or immune cell differentiation and 8 housekeeping genes were studied as described previously (18). The quantifications were performed using the Biomark microfluidic system from Fluidigm (GeT-PlaGe platform, France), in which every sample-gene combination is quantified using a 96.96 Dynamic Array IFC (integrated fluidic circuit) (product number bBMK-M-96.96; Fluidigm). Specific target amplification (STA) was performed on the 80 cDNA samples, an internal control (genomic DNA), a negative control (Tris-EDTA [TE]), a bovine genomic DNA control, and pooled cDNAs of the 80 cDNA samples in 5-fold serial dilutions (to determine the PCR amplification efficiency). Each sample was preamplified with a pool of selected primer pairs (0.2  $\mu$ M each primer) in a thermocycler with an initial activation step (95°C for 10 min) followed by 16 cycles of two amplification steps (95°C for 15 s and 60°C for 4 min). The free primers present in the preamplification products were digested with an exonuclease (NEB, MA, USA) before the samples were diluted in TE with a 1:5 dilution factor. The preamplification, digested, and diluted products were prepared with 50% 2 $\times$  TaqMan gene expression master mix (Applied Biosystems, CA, USA), 5% 20 $\times$  DNA binding dye sample loading reagent (Fluidigm, CA, USA), 5% EvaGreen (Interchim, France), and 15% 1 $\times$  TE in a 10- $\mu$ l final volume. The BioMark 96.96 Dynamic Array chip (Fluidigm, CA, USA) was loaded with 5  $\mu$ l of each prepared sample. Gene expression levels were measured after 35 cycles on the BioMark HD real-time PCR system. The quality control was checked by using the Fluidigm software (Fluidigm, CA, USA).

A clean data set was obtained after analysis of the melting curves using Fluidigm real-time PCR analysis software version 4.1.3. As a standard, a pool of the 80 cDNA samples was used in five serial dilutions to determine the gene amplification efficiencies (Eff). Genes with amplification efficiencies lower than 1.7 or higher than 2.2 and genes with fewer than three of the five standard points amplified were removed from the analysis.

The relative gene expression (RE) for each sample was calculated as proposed by Pfaffl (53) with the equation  $RE_{(gene)} = Eff_{(gene)}^{-(CT_{calibrator} - CT_{sample})}$ , where *CT* is cycle threshold and the calibrator is the first point of the standard curve (Table S2). GeNorm was used to choose the four most stable housekeeping genes. The select HKgenes function with the Vandesompele method (54) of the SLqPCR package was used with RStudio (version 1.2.1335). Finally, the relative expression level for each sample was normalized for the geometric average expression of the selected housekeeping genes as follows:

$$\text{normalized } RE_{(gene)} = RE_{(gene)} / \sqrt[3]{(RE_{(RPL19)} \times RE_{(RPL26)} \times RE_{(SOD2)} \times RE_{(YWHA7)})}$$

A cutoff was chosen to only select genes with less than 40% missing values. In total, 52 of 76 genes were retained for this study. The normalized relative expression of these 52 genes was log transformed, and missing values were imputed using the missMDA package of R software.

**Bovine IFN- $\gamma$  quantification.** The concentrations of bovine IFN- $\gamma$  in BAL fluid samples were measured by using a homemade sandwich ELISA. The mouse anti-bovine IFN- $\gamma$  antibody (clone CC330, catalog number MCA2112; Bio-Rad) was incubated on ELISA plates (MaxiSorp; Nunc, Denmark) for 18 h at 4°C using 100 ng per well in 100  $\mu$ l coating buffer containing 0.05 M Na-carbonate bicarbonate, pH 9.6. After three washes with 100  $\mu$ l of wash buffer (PBS containing 0.05% Tween 20), wells were blocked for 1 h at room temperature with 100  $\mu$ l of PBS containing 1% bovine serum albumin (BSA). After three washes, 100  $\mu$ l of 1:2-diluted BAL fluid samples were added. A standard range was done using the recombinant bovine IFN- $\gamma$  (catalog number PBPO07A; Bio-Rad) diluted in wash buffer at a final concentration between 0.0125 and 125 ng/ml. After incubation overnight at 4°C and three washes, 100  $\mu$ l of biotinylated mouse anti-bovine IFN- $\gamma$  antibody (clone CC302, catalog number MCA1783B; Bio-Rad) labeled with streptavidin-HRP was added to each well. After incubation at 37°C for 1 h, the ELISA plates were washed three times. Absorbance was read at 450 nm on the CLARIOstar microplate reader (BMG Labtech) after the addition of 100  $\mu$ l HRP substrate (Bio-Rad).

**Statistical analysis.** Statistical analysis for clinical, serological, and virological analyses was performed using GraphPad (La Jolla, CA, USA). Logarithmic transformation was applied to fulfill the conditions of variances in homogeneity and normality when necessary (qPCR data). Data were expressed as arithmetic mean values  $\pm$  standard errors of the means (SEM). A two-way analysis of variance (ANOVA) with repeated measures (3-factor split-plot ANOVA) was used to analyze the clinical, ELISA, and qPCR results. When effects of the "day" and "treatment" factors were significant among interactions, a Bonferroni test between contrasts was used to compare the treatments on each day postchallenge. A one-way ANOVA was used to compare the means of the individual areas under daily clinical scores (ACS). When the effect of the "treatment" factor was significant, a Newman-Keuls test was used to

compare the treatment effects at each time point. A *t* test (Mann-Whitney test) was also run for these parameters.

Statistical analyses of the DEGs between samples at the different stages of infection (2, 7, and 14 dpi) were obtained using R Studio software. Data for each sample were analyzed with a linear model that used the animal as a random parameter and the type of infection as a fixed parameter. Correction for multiple testing was performed with the estimation of false discovery rate as proposed by Benjamini and Hochberg (55). After correction, differentially expressed genes with a significant difference ( $P < 0.05$ ) were identified. Finally, for each comparison, the fold change was calculated and represented.

## SUPPLEMENTAL MATERIAL

Supplemental material is available online only.

**SUPPLEMENTAL FILE 1**, XLSX file, 0.02 MB.

**SUPPLEMENTAL FILE 2**, XLSX file, 0.1 MB.

## ACKNOWLEDGMENTS

This work was funded by the Agence Nationale pour la Recherche (ANR) via project number ANR-15-CE35-0005 FLUD.

We thank David Gauthier and Edouard Guitton for their work in the animal facility and Sandra Fourre of the GeT-PlaGe platform (Toulouse) and Charlotte Foret-Lucas for their assistance in the Fluidigm experiments. We also thank Julie Cournet-Brousseau, Nathan Cebron, and Gilles Foucras for their valuable scientific support and for their help with the KingFisher flex purification system.

## REFERENCES

- Taylor JD, Fulton RW, Lehenbauer TW, Step DL, Confer AW. 2010. The epidemiology of bovine respiratory disease: what is the evidence for predisposing factors? *Can Vet J* 51:1095–1102.
- Grissett GP, White BJ, Larson RL. 2015. Structured literature review of responses of cattle to viral and bacterial pathogens causing bovine respiratory disease complex. *J Vet Intern Med* 29:770–780. <https://doi.org/10.1111/jvim.12597>.
- Lhermie G, Ferran AA, Assié S, Cassard H, El Garch F, Schneider M, Woerhlé F, Pacalin D, Delverdier M, Bousquet-Mélou A, Meyer G. 2016. Impact of timing and dosage of a fluoroquinolone treatment on the microbiological, pathological, and clinical outcomes of calves challenged with *Mannheimia haemolytica*. *Front Microbiol* 7:237. <https://doi.org/10.3389/fmicb.2016.00237>.
- Blodörn K, Hägglund S, Gavner-Widen D, Eléouët J-F, Riffault S, Pringle J, Taylor G, Valarcher JF. 2015. A bovine respiratory syncytial virus model with high clinical expression in calves with specific passive immunity. *BMC Vet Res* 11:76. <https://doi.org/10.1186/s12917-015-0389-6>.
- Zhang M, Hill JE, Alexander TW, Huang Y. 2021. The nasal viromes of cattle on arrival at western Canadian feedlots and their relationship to development of bovine respiratory disease. *Transbound Emerg Dis* 68:2209–2218. <https://doi.org/10.1111/tbed.13873>.
- Zhang M, Hill JE, Fernando C, Alexander TW, Timsit E, van der Meer F, Huang Y. 2019. Respiratory viruses identified in western Canadian beef cattle by metagenomic sequencing and their association with bovine respiratory disease. *Transbound Emerg Dis* 66:1379–1386. <https://doi.org/10.1111/tbed.13172>.
- Mitra N, Cernicchiaro N, Torres S, Li F, Hause BM. 2016. Metagenomic characterization of the virome associated with bovine respiratory disease in feedlot cattle identified novel viruses and suggests an etiologic role for influenza D virus. *J Gen Virol* 97:1771–1784. <https://doi.org/10.1099/jgv.0.000492>.
- Ng TFF, Kondov NO, Deng X, Van Eenennaam A, Neiberghs HL, Delwart E. 2015. A metagenomics and case-control study to identify viruses associated with bovine respiratory disease. *J Virol* 89:5340–5349. <https://doi.org/10.1128/JVI.00064-15>.
- Ducatez MF, Pelletier C, Meyer G. 2015. Influenza D virus in cattle, France, 2011–2014. *Emerging Infect Dis* 21:368–371.
- Hause BM, Ducatez M, Collin EA, Ran Z, Liu R, Sheng Z, Armién A, Kaplan B, Chakravarty S, Hoppe AD, Webby RJ, Simonson RR, Li F. 2013. Isolation of a novel swine influenza virus from Oklahoma in 2011 which is distantly related to human influenza C viruses. *PLoS Pathog* 9:e1003176. <https://doi.org/10.1371/journal.ppat.1003176>.
- Luo J, Ferguson L, Smith DR, Woolums AR, Epperson WB, Wan X-F. 2017. Serological evidence for high prevalence of influenza D viruses in cattle, Nebraska, United States, 2003–2004. *Virology* 501:88–91. <https://doi.org/10.1016/j.virol.2016.11.004>.
- O'Donovan T, Donohoe L, Ducatez MF, Meyer G, Ryan E. 2019. Seroprevalence of influenza D virus in selected sample groups of Irish cattle, sheep and pigs. *Ir Vet J* 72:11. <https://doi.org/10.1186/s13620-019-0150-8>.
- Oliva J, Eichenbaum A, Belin J, Gaudino M, Guillotin J, Alzieu J-P, Nicolle P, Brugidou R, Gueneau E, Michel E, Meyer G, Ducatez MF. 2019. Serological evidence of influenza D virus circulation among cattle and small ruminants in France. *Viruses* 11:516. <https://doi.org/10.3390/v11060516>.
- Rosignoli C, Faccini S, Merenda M, Chiapponi C, de Mattia A, Bufalo G, Garbarino C, Baioni L, Bolzoni L, Nigrelli A, Foni E. 2017. Influenza D virus infection in cattle in Italy. *Large Animal Rev* 23:123–128.
- Fusade-Boyer M, Pato PS, Komlan M, Dogno K, Batawui K, Go-Maró E, McKenzie P, Guinat C, Secula A, Paul M, Webby RJ, Tran A, Waret-Szkuta A, Ducatez MF. 2020. Risk mapping of influenza D virus occurrence in ruminants and swine in Togo using a spatial multicriteria decision analysis approach. *Viruses* 12:128. <https://doi.org/10.3390/v12020128>.
- Snoeck CJ, Oliva J, Pauly M, Losch S, Wildschutz F, Muller CP, Hübschen JM, Ducatez MF. 2018. Influenza D virus circulation in cattle and swine, Luxembourg, 2012–2016. *Emerg Infect Dis* 24:1388–1389. <https://doi.org/10.3201/eid2407.171937>.
- Ferguson L, Olivier AK, Genova S, Epperson WB, Smith DR, Schneider L, Barton K, McCuan K, Webby RJ, Wan X-F. 2016. Pathogenesis of influenza D virus in cattle. *J Virol* 90:5636–5642. <https://doi.org/10.1128/JVI.03122-15>.
- Salem E, Hägglund S, Cassard H, Corre T, Näslund K, Foret C, Gauthier D, Pinard A, Delverdier M, Zohari S, Valarcher J-F, Ducatez M, Meyer G. 2019. Pathogenesis, host innate immune response, and aerosol transmission of influenza D virus in cattle. *J Virol* 93:e01853-18. <https://doi.org/10.1128/JVI.01853-18>.
- Hament J-M, Kimpen JLL, Fleer A, Wolfs TFW. 1999. Respiratory viral infection predisposing for bacterial disease: a concise review. *FEMS Immunol Med Microbiol* 26:189–195. <https://doi.org/10.1111/j.1574-695X.1999.tb01389.x>.
- McCullers JA. 2014. The co-pathogenesis of influenza viruses with bacteria in the lung. *Nat Rev Microbiol* 12:252–262. <https://doi.org/10.1038/nrmicro3231>.
- Rynda-Apple A, Robinson KM, Alcorn JF. 2015. Influenza and bacterial superinfection: illuminating the immunologic mechanisms of disease. *Infect Immun* 83:3764–3770. <https://doi.org/10.1128/IAI.00298-15>.
- Bakaletz LO. 2017. Viral-bacterial co-infections in the respiratory tract. *Curr Opin Microbiol* 35:30–35. <https://doi.org/10.1016/j.mib.2016.11.003>.



23. Saegerman C, Gaudino M, Savard C, Broes A, Ariel O, Meyer G, Ducatez MF. 2021. Influenza D virus in respiratory disease in Canadian, province of Québec, cattle: relative importance and evidence of new reassortment between different clades. *Transbound Emerg Dis*. <https://doi.org/10.1111/tbed.14085>.
24. Caswell JL, Bateman KG, Cai HY, Castillo-Alcala F. 2010. *Mycoplasma bovis* in respiratory disease of feedlot cattle. *Vet Clin North Am Food Anim Pract* 26:365–379. <https://doi.org/10.1016/j.cvfa.2010.03.003>.
25. Oliveira TES, Pelaquim IF, Flores EF, Massi RP, Valdiviezo MJJ, Pretto-Giordano LG, Alfieri AA, Saut JPE, Headley SA. 2020. *Mycoplasma bovis* and viral agents associated with the development of bovine respiratory disease in adult dairy cows. *Transbound Emerg Dis* 67(Suppl 2):82–93. <https://doi.org/10.1111/tbed.13223>.
26. Zhang X, Outlaw C, Olivier AK, Woolums A, Epperson W, Wan X-F. 2019. Pathogenesis of co-infections of influenza D virus and *Mannheimia haemolytica* in cattle. *Vet Microbiol* 231:246–253. <https://doi.org/10.1016/j.vetmic.2019.03.027>.
27. Prysiak T, van der Merwe J, Lawman Z, Wilson D, Townsend H, van Druenen Littel-van den Hurk S, Perez-Casal J. 2011. Respiratory disease caused by *Mycoplasma bovis* is enhanced by exposure to bovine herpes virus 1 (BHV-1) but not to bovine viral diarrhoea virus (BVDV) type 2. *Can Vet J* 52:1195–1202.
28. Oliva J, Mettler J, Sedano L, Delverdier M, Bourgès-Abella N, Hause B, Loupias J, Pardo I, Bleuart C, Bordignon PJ, Meunier E, Le Goffic R, Meyer G, Ducatez MF. 2020. Murine model for the study of influenza D virus. *J Virol* 94:e01662-19. <https://doi.org/10.1128/JVI.01662-19>.
29. Chao J, Han X, Liu K, Li Q, Peng Q, Lu S, Zhu X, Hu G, Dong Y, Hu C, Chen Y, Chen J, Khan FA, Chen H, Guo AA. 2019. Calves infected with virulent and attenuated *Mycoplasma bovis* strains have upregulated Th17 inflammatory and Th1 protective responses, respectively. *Genes* 10:656. <https://doi.org/10.3390/genes10090656>.
30. Kanci A, Wawegama NK, Marendra MS, Mansell PD, Browning GF, Markham PF. 2017. Reproduction of respiratory mycoplasmosis in calves by exposure to an aerosolised culture of *Mycoplasma bovis*. *Vet Microbiol* 210:167–173. <https://doi.org/10.1016/j.vetmic.2017.09.013>.
31. Stipkovits L, Ripley PH, Tenk M, Glávits R, Molnár T, Fodor L. 2005. The efficacy of valnemulin (Econor) in the control of disease caused by experimental infection of calves with *Mycoplasma bovis*. *Res Vet Sci* 78:207–215. <https://doi.org/10.1016/j.rvsc.2004.09.005>.
32. Nicholas RAJ, Ayling RD, Stipkovits LP. 2002. An experimental vaccine for calf pneumonia caused by *Mycoplasma bovis*: clinical, cultural, serological and pathological findings. *Vaccine* 20:3569–3575. [https://doi.org/10.1016/S0264-410X\(02\)00340-7](https://doi.org/10.1016/S0264-410X(02)00340-7).
33. Sun K, Metzger DW. 2008. Inhibition of pulmonary antibacterial defense by interferon- $\gamma$  during recovery from influenza infection. *Nat Med* 14:558–564. <https://doi.org/10.1038/nm1765>.
34. Robinson KM, Kolls JK, Alcorn JF. 2015. The immunology of influenza virus-associated bacterial pneumonia. *Curr Opin Immunol* 34:59–67. <https://doi.org/10.1016/j.coi.2015.02.002>.
35. Ghoneim HE, Thomas PG, McCullers JA. 2013. Depletion of alveolar macrophages during influenza infection facilitates bacterial superinfections. *J Immunol* 191:1250–1259. <https://doi.org/10.4049/jimmunol.1300014>.
36. Skelton RM, Shepardson KM, Hattori A, Wilson PT, Sreenivasan C, Yu J, Wang D, Huber VC, Rynda-Apple A. 2019. Contribution of host immune responses against influenza D virus infection toward secondary bacterial infection in a mouse model. *Viruses* 11:994. <https://doi.org/10.3390/v11110994>.
37. Kudva A, Scheller EV, Robinson KM, Crowe CR, Choi SM, Slight SR, Khader SA, Dubin PJ, Enelow RI, Kolls JK, Alcorn JF. 2011. Influenza A inhibits Th17-mediated host defense against bacterial pneumonia in mice. *J Immunol* 186:1666–1674. <https://doi.org/10.4049/jimmunol.1002194>.
38. Danjanovic D, Lai R, Jeyanathan M, Hogaboam CM, Xing Z. 2013. Marked improvement of severe lung immunopathology by influenza-associated pneumococcal superinfection requires the control of both bacterial replication and host immune responses. *Am J Pathol* 183:868–880. <https://doi.org/10.1016/j.ajpath.2013.05.016>.
39. Califano D, Furuya Y, Metzger DW. 2018. Effects of influenza on alveolar macrophage viability are dependent on mouse genetic strain. *J Immunol* 201:134–144. <https://doi.org/10.4049/jimmunol.1701406>.
40. Macpherson AJ, McCoy KD, Johansen F-E, Brandtzaeg P. 2008. The immune geography of IgA induction and function. *Mucosal Immunol* 1:11–22. <https://doi.org/10.1038/mi.2007.6>.
41. Renegar KB, Small PA, Boykins LG, Wright PF. 2004. Role of IgA versus IgG in the control of influenza viral infection in the murine respiratory tract. *J Immunol* 173:1978–1986. <https://doi.org/10.4049/jimmunol.173.3.1978>.
42. Hijano DR, Siefker DT, Shrestha B, Jaligama S, Vu LD, Tillman H, Finkelstein D, Saravia J, You D, Cormier SA. 2018. Type I interferon potentiates IgA immunity to respiratory syncytial virus infection during infancy. *Sci Rep* 8:11034. <https://doi.org/10.1038/s41598-018-29456-w>.
43. Feldmann A, Schäfer MK-H, Garten W, Klenk H-D. 2000. Targeted infection of endothelial cells by avian influenza virus A/FPV/Rostock/34 (H7N1) in chicken embryos. *J Virol* 74:8018–8027. <https://doi.org/10.1128/jvi.74.17.8018-8027.2000>.
44. Horimoto T, Nakayama K, Smeekens SP, Kawaoka Y. 1994. Proprotein-processing endoproteases PC6 and furin both activate hemagglutinin of virulent avian influenza viruses. *J Virol* 68:6074–6078. <https://doi.org/10.1128/JVI.68.9.6074-6078.1994>.
45. Limburg H, Harbig A, Bestle D, Stein DA, Moulton HM, Jaeger J, Janga H, Hards K, Koepke J, Schulte L, Koczulla AR, Schmeck B, Klenk H-D, Böttcher-Friebertshäuser E. 2019. TMPRSS2 is the major activating protease of influenza A virus in primary human airway cells and influenza B virus in human type II pneumocytes. *J Virol* 93:22. <https://doi.org/10.1128/JVI.00649-19>.
46. Chaipan C, Kobasa D, Bertram S, Glowacka I, Steffen I, Solomon Tsegaye T, Takeda M, Bugge TH, Kim S, Park Y, Marzi A, Pöhlmann S. 2009. Proteolytic activation of the 1918 influenza virus hemagglutinin. *J Virol* 83:3200–3211. <https://doi.org/10.1128/JVI.02205-08>.
47. Su S, Fu X, Li G, Kerlin F, Veit M. 2017. Novel influenza D virus: epidemiology, pathology, evolution and biological characteristics. *Virulence* 8:1580–1591. <https://doi.org/10.1080/21505594.2017.1365216>.
48. Zhu X, Dordet-Frisoni E, Gillard L, Ba A, Hygonenq M-C, Sagné E, Nouvel LX, Maillard R, Assié S, Guo A, Citti C, Baranowski E. 2019. Extracellular DNA: a nutritional trigger of *Mycoplasma bovis* cytotoxicity. *Front Microbiol* 10:2753. <https://doi.org/10.3389/fmicb.2019.02753>.
49. Tully JG. 1995. Culture medium formulation for primary isolation and maintenance of Mollicutes, p 33–39. *In* Razin S, Tully JG (ed), *Molecular and diagnostic procedures in mycoplasmaology: molecular characterization*. Academic Press, San Diego, CA.
50. European Parliament and Council of the European Union. 2010. Directive 2010/63/EU of the European Parliament and of the Council of 22 September 2010 on the protection of animals used for scientific purposes. *Off J Eur Union L* 33:34–79.
51. Alvarez IJ, Fort M, Pasucci J, Moreno F, Gimenez H, Näslund K, Hägglund S, Zohari S, Valarcher JF. 2020. Seroprevalence of influenza D virus in bulls in Argentina. *J Vet Diagn Invest* 32:585–588. <https://doi.org/10.1177/1040638720934056>.
52. Uttenthal A, Larsen LE, Philipsen JS, Tjørnehøj K, Viuff B, Nielsen KH, Nielsen TK. 2000. Antibody dynamics in BRSV-infected Danish dairy herds as determined by isotype-specific immunoglobulins. *Vet Microbiol* 76:329–341. [https://doi.org/10.1016/S0378-1135\(00\)00261-3](https://doi.org/10.1016/S0378-1135(00)00261-3).
53. Pfaffl MW. 2001. A new mathematical model for relative quantification in real-time RT-PCR. *Nucleic Acids Res* 29:e45. <https://doi.org/10.1093/nar/29.9.e45>.
54. Vandesompele J, De Preter K, Pattyn F, Poppe B, Van Roy N, De Paeppe A, Speleman F. 2002. Accurate normalization of real-time quantitative RT-PCR data by geometric averaging of multiple internal control genes. *Genome Biol* 3:RESEARCH0034. <https://doi.org/10.1186/gb-2002-3-7-research0034>.
55. Benjamini Y, Hochberg Y. 1995. Controlling the false discovery rate: a practical and powerful approach to multiple testing. *J R Stat Soc Series B Stat Methodol* 57:289–300. <https://doi.org/10.1111/j.2517-6161.1995.tb02031.x>.